



Synthesis and biological evaluation of novel chromonyl enamines as α -glucosidase inhibitors

Aarón Mendieta-Moctezuma^{1,2} · Catalina Rugerio-Escalona¹ · Nemesio Villa-Ruano³ · Rsuini U. Gutierrez² · Fabiola E. Jiménez-Montejo¹ · M. Jonathan Fragoso-Vázquez⁴ · José Correa-Basurto⁴ · María C. Cruz-López¹ · Francisco Delgado² · Joaquín Tamariz²

Received: 20 December 2018 / Accepted: 21 February 2019
© Springer Science+Business Media, LLC, part of Springer Nature 2019

Abstract

Series of novel chromonyl enamines **1a–e** and **2a–e** and 3-alkylated chromones **3a–e** were synthesized and evaluated in vitro as α -glucosidase inhibitors as well as antioxidant and antifungal agents. Antifungal activity was tested on strains of *Candida albicans*. Compounds **2a** and **2d–e** showed good inhibition of the α -glucosidase enzyme ($IC_{50} = 5.5, 0.9, \text{ and } 1.5$ mM, respectively), their effect being better than that of **1a–e**, **3a–e**, and acarbose (the standard, $IC_{50} = 7.73 \pm 0.9$ mM). The structure–activity relationship suggests that the phenyl group at the C-3 position of the chromone ring system and the 4-chlorophenyl group at the enamine moiety (derivatives **2**) increased the inhibition of α -glucosidase. Compounds **2a–e** exhibited a slight antioxidant effect, and compounds **3a–e** a moderate antifungal activity against *C. albicans* (IC_{50} 70.5–83.1 $\mu\text{g/mL}$). Docking studies revealed that compounds **2** interact with the α -glucosidase residues of the binding pocket. Therefore, these chromone derivatives may be considered as potential α -glucosidase inhibitors, as well as antifungal agents against some *Candida* strains of yeast.

Keywords Chromonyl enamines · Chromones · α -glucosidase inhibitors · *Candida albicans*

Supplementary information The online version of this article (<https://doi.org/10.1007/s00044-019-02320-w>) contains supplementary material, which is available to authorized users.

- ✉ Aarón Mendieta-Moctezuma
amendietam@ipn.mx
- ✉ Joaquín Tamariz
jtamarizm@ipn.mx
jtamariz@woodward.enb.ipn.mx

- ¹ Centro de Investigación en Biotecnología Aplicada, Instituto Politécnico Nacional, Carretera Estatal Santa Inés Tecuexcomac-Tepetitla, Km 1.5, 90700 Tlaxcala, Mexico
- ² Departamento de Química Orgánica, Escuela Nacional de Ciencias Biológicas, Instituto Politécnico Nacional, Prol. Carpio y Plan de Ayala S/N, 11340 Ciudad de México, Mexico
- ³ Universidad de la Sierra Sur, Ciudad Universitaria, Guillermo Rojas Mijangos S/N, Miahuatlán de Porfirio Díaz, 70800 Oaxaca, Mexico
- ⁴ Laboratorio de Desarrollo de Fármacos y Productos Biotecnológicos, Escuela Superior de Medicina, Instituto Politécnico Nacional, Plan de San Luis y Díaz Mirón S/N, 11340 Ciudad de México, Mexico

Introduction

Heterocycles are very important molecular components for drug design and discovery (Keri et al. 2014). Chromones are oxygenated heterocyclic compounds with a benzo-annulated γ -pyrone ring (4*H*-chromen-4-one, 4*H*-1-benzopyran-one) that are present in numerous naturally occurring and synthetic compounds. They are well-known for their wide range of pharmacological activity, including antimicrobial (Dofe et al. 2017a, b), antitumor (Sun et al. 2013), cytotoxic (Xiu et al. 2017), antioxidant (Csepanyi et al. 2017), anti-HIV (Kim et al. 2013), anti-inflammatory (Gaspar et al. 2014), and anti-diabetes (Reis et al. 2017).

There are various reports on chromone derivatives as potent α -glucosidase inhibitors (Philip et al. 2017; Zhen et al. 2017; Wang et al. 2017, 2018; Jose et al. 2018). Previous docking and structure–activity relationship (SAR) studies suggest that binding with the α -glucosidase enzyme is favored (thus increasing inhibition) by the inclusion of a tertiary amino group and an aromatic ring substituted with a hydrogen acceptor at the C-6 or C-7 position of the chromone ring (Zhen et al. 2017; Wang et al. 2018). Hence,

modifications in the structure of this type of compound offer an alternative in the search for novel therapeutic agents.

Type 2 diabetes is caused by hyperglycemia in the blood due to a scarce production or malfunction of insulin, which can also lead to serious complications of the heart, blood vessels, nerves, kidney, and eyes. One therapeutic treatment for diabetes is to delay glucose absorption by inhibiting digestive enzymes such as amylases and glucosidases (Kerru et al. 2018). α -Glucosidase inhibitors, which include acarbose, miglitol, and voglibose, are first-line drugs for the treatment of type-2 diabetes because they decrease postprandial hyperglycemia (Wang et al. 2017; Upadhyay et al. 2018). However, the drugs currently used for controlling type 2 diabetes have many negative side effects (Upadhyay et al. 2018). In the search for safer and more efficient inhibitors, new drugs have been designed and developed to control diabetes (Kerru et al. 2018).

One of the complications associated with diabetes is the susceptibility of contracting infections by opportunistic microorganisms, especially yeasts of the genus *Candida* (Brunel and Guery 2017). When sugar levels are elevated, diabetic patients tend to be more susceptible, although the mechanisms involved have not been fully elucidated. It appears that hyperglycemia suppresses the immune system of the diabetic patient, thus fostering an increased prevalence of infections by drug-resistant pathogens. The synthesis of new compounds to cope with microbial resistance to antibiotics has become an urgent priority for medicinal chemistry (Dofe et al. 2017a, b; Reis et al. 2017), highlighting the need for novel and more effective drugs (Brunel and Guery 2017; Jose et al. 2018). To meet this challenge, it is possible to modify existing molecules or design new ones in accordance with the therapeutic targets.

For the development of potent and efficient molecules with biological activity, the chromone and flavonoid scaffolds are important to consider (Reis et al. 2017; Lu et al. 2017). We herein describe the design and synthesis of a hybrid scaffold that incorporates chromone and enaminone moieties in a single molecule mimicking the structure of known α -glucosidase inhibitors (Fig. 1) (Zhen et al. 2017; Wang et al. 2018). The synthesized compounds were evaluated for α -glucosidase inhibition as well as antioxidant and antifungal activity. The most promising compounds in

the experimental assays (**2a**, **2d**, and **2e**) were subjected to docking studies on α -glucosidase in order to explore their recognition properties.

Materials and methods

Chemistry

Melting points were determined on an electrothermal apparatus and are uncorrected. ^1H (300 or 500 MHz) and ^{13}C (75 or 125 MHz) NMR spectra were recorded on a Varian Mercury-300 or Varian VNMR system instrument. The chemical shifts (δ) are expressed in ppm relative to the TMS as the internal standard. Mass spectra were obtained (in electron impact (EI) mode) on a Polaris Q-Trace GC Ultra/Finnigan Co apparatus, and the high-resolution mass spectra (HRMS, in EI), were obtained on a Jeol JSM-GCMatell instrument. Infrared spectra (IR) were recorded on a FT-IR 2000 Perkin-Elmer spectrometer. Elemental analyses were performed on a CE-440 Exeter Analytical apparatus. Commercial reagents were employed as received from Sigma-Aldrich and anhydrous solvents were obtained by a distillation process. Thin layer chromatography was carried out on precoated silica gel plates (Merck 60F₂₅₄). Silica gel (230–400 mesh) was used for flash column chromatography. The preparation of compounds **4a–c**, **6a–6c**, **6e**, **7a–b**, **7d**, and **8a–8b** has been previously described (Mendieta et al. 2014; Musso et al. 2010; Huls 1958; Zoe et al. 2010; Jha et al. 1981; Goto et al. 2009; Rao and Krupadanam 1994; Moore et al. 1934).

General procedure for the synthesis of 2-acyl phenols 6–8

$\text{BF}_3\cdot\text{OEt}_2$ (1.0 mol equiv.) was added to a solution of phenols **9a–c** (2.0 mol equiv. for **9a–b** and 1.0 mol equiv. for **9c**) and the corresponding acyl chloride (2.0 mol equiv.) under nitrogen atmosphere at 0 °C. The mixture was then stirred at 80 °C for 3 h. After pouring the residue into ice water (10 mL), adjusted to neutral pH with an aqueous saturated solution of NaHCO_3 , and extracted with EtOAc (3 \times 30 mL). The organic layer was dried over Na_2SO_4 and concentrated under reduced pressure, followed by purifying

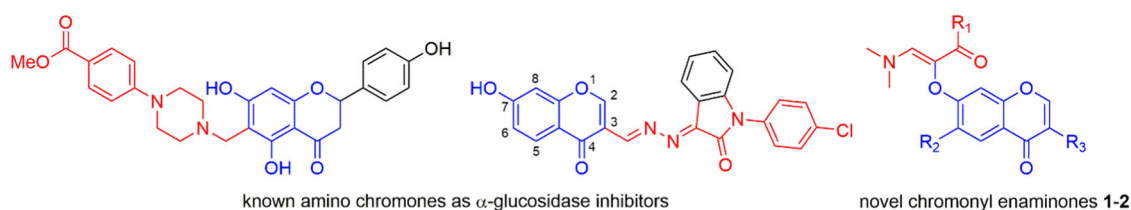


Fig. 1 Structures of known flavanone and chromone as α -glucosidase inhibitors, and the novel chromone-enaminones **1–2** herein described

the residue by column chromatography over silica gel (hexane/EtOAc, 9:1) to give the respective acyl phenols **6–8** (Mendieta et al. 2014).

1-(2-Hydroxy-4,5-dimethoxyphenyl)ethanone (6a) White solid (88%). *Rf* 0.20 (hexane/EtOAc, 8:2); mp 106–107 °C (Lit. 107–108 °C, Mendieta et al. 2014).

1-(2-Hydroxy-4,5-dimethoxyphenyl)propan-1-one (6b) White solid (92%). *Rf* 0.34 (hexane/EtOAc, 8:2); mp 124–125 °C (Lit. 118–119 °C, Musso et al. 2010).

1-(2-Hydroxy-4,5-dimethoxyphenyl)butan-1-one (6c) Colorless solid (85%). *Rf* 0.25 (hexane/EtOAc, 8:2); mp 77–78 °C (Lit. 76–77 °C, Mendieta et al. 2014).

1-(2-Hydroxy-4,5-dimethoxyphenyl)pentan-1-one (6d) Yellow solid (88%). *Rf* 0.37 (hexane/EtOAc, 8:2); mp 93–94 °C; IR (KBr) ν_{\max} : 2955, 2869, 1629, 1582, 1510, 1390, 1270, 1249, 1196, 1156 cm^{-1} ; ^1H NMR (500 MHz, CDCl_3) δ : 0.97 (m, 3H, CH_3 , H-5), 1.43 (m, 2H, CH_2 , H-4), 1.72 (m, 2H, CH_2 , H-3), 2.88 (q, $J = 7.2$ Hz, 2H, CH_2 , H-2), 3.86 (s, 3H, OCH_3 -C₅), 3.90 (s, 3H, OCH_3 -C₄), 6.45 (s, 1H, H-3'), 7.09 (s, 1H, H-6'), 12.78 (s, 1H, OH); ^{13}C NMR (125 MHz, CDCl_3) δ : 13.8 (CH_3 -5), 22.4 (CH_2 -4), 26.6 (CH_2 -3), 37.7 (CH_2 -2), 56.0 (OCH_3 -4'), 56.6 (OCH_3 -5'), 100.5 (C-3'), 111.1 (C-1'), 111.2 (C-6'), 141.7 (C-5'), 156.5 (C-4'), 160.1 (C-2'), 204.5 (CO); MS (70 eV) m/z 238 (M^+ , 36), 209 (14), 196 (45), 181 (100), 125 (33), 110 (11), 95 (10), 55 (14). HMRS (70 eV) Calculated for: $\text{C}_{13}\text{H}_{18}\text{O}_4$. 238.1205. Found: 238.1199.

1-(2-Hydroxy-4,5-dimethoxyphenyl)-3-methylbutan-1-one (6e) Yellow solid (84%). *Rf* 0.40 (hexane/EtOAc, 8:2); mp 60–61 °C (Lit. 62 °C, Huls 1958).

1-(2,4-Dihydroxy-5-methoxyphenyl)ethan-1-one (7a) White solid (86%). *Rf* 0.49 (hexane/EtOAc, 6:4); mp 171–172 °C (Lit. 170–171 °C, Zou et al. 2010).

1-(2,4-Dihydroxy-5-methoxyphenyl)propan-1-one (7b) White solid (80%). *Rf* 0.51 (hexane/EtOAc, 6:4); mp 124–125 °C (lit mp not given, Jha et al. 1981).

1-(2,4-Dihydroxy-5-methoxyphenyl)butan-1-one (7c) White solid (85%). *Rf* 0.57 (hexane/EtOAc, 6:4); mp 98–99 °C. IR (KBr) ν_{\max} : 3303, 2962, 1637, 1600, 1510, 1430, 1374, 1302, 1226, 1201, 1164, 1025, 838, 741, 675 cm^{-1} ; ^1H NMR (500 MHz, CDCl_3) δ : 1.03 (t, $J = 7.5$ Hz, 3H, CH_3 , H-4), 1.78 (sext, t, $J = 7.5$ Hz, 2H, CH_2 , H-3), 2.86 (t, $J = 7.5$ Hz, 2H, CH_2 , H-2), 3.90 (s, 3H, OCH_3), 6.34 (s, 1H, OH-4'), 6.51 (s, 1H, H-3'), 7.08 (s, 1H, H-6'), 12.73 (s, 1H, OH-2'); ^{13}C NMR (125 MHz, CDCl_3) δ : 13.9 (CH_3 -C₄), 18.0 (CH_2 -C₃), 39.9

(CH_2 -C₂), 56.5 (OCH_3), 103.6 (C-3'), 110.2 (C-6'), 111.7 (C-1'), 139.7 (C-5'), 153.5 (C-4'), 160.3 (C-2'), 204.2 (CO); MS (70 eV) m/z 210 (M^+ , 35), 195 (7), 182 (10), 167 (100), 152 (10), 111 (11). HRMS (70 eV) Calculated for: $\text{C}_{11}\text{H}_{14}\text{O}_4$. 210.0892. Found: 210.0886.

1-(2,4-Dihydroxy-5-methoxyphenyl)-2-phenylethan-1-one (7d) White solid (50%). *Rf* 0.34 (hexane/EtOAc, 6:4); mp 91–92 °C (Lit. 88–89 °C, Goto et al. 2009).

1-(5-Chloro-2,4-dihydroxyphenyl)propan-1-one (8a) White solid (99%). *Rf* 0.75 (hexane/EtOAc, 6:4); mp 101–102 °C (Lit. 90 °C, Rao and Krupadanam 1994).

1-(5-Chloro-2,4-dihydroxyphenyl)butan-1-one (8b) White solid (90%). *Rf* 0.31 (hexane/EtOAc, 8:2); mp 91–92 °C (Lit. 84–85 °C, Moore et al. 1934).

General procedure for the synthesis of aryloxycarbonylic compounds 4–5

A solution of acyl phenols **7** and **8** (1.0 mol equiv.) and K_2CO_3 (1.5 mol equiv.) in dry acetone (7 mL) was stirred at 25 °C for 15 min. Subsequently, the corresponding α -halo-carbonyl compound **11a–b** (1.5 mol equiv.) was added dropwise and the reaction mixture was refluxed at 60 °C for 3 h. After the reaction was completed (according to TLC monitoring), the mixture was filtered, and the solvent removed over vacuum. The residue was purified by flash chromatography to give the respective compounds **4** and **5** (Jiménez et al. 2010).

Methyl 2-(4-acetyl-5-hydroxy-2-methoxyphenoxy)acetate (4a) White solid (90%). *Rf* 0.30 (hexane/EtOAc 6:4); mp 133–134 °C (Lit. 132–133 °C, Mendieta et al. 2014).

Methyl 2-(5-hydroxy-2-methoxy-4-propionylphenoxy)acetate (4b) White solid (97%). *Rf* 0.5 (hexano/EtOAc 6:4); mp 119–121 °C (Lit. 119–120 °C, Mendieta et al. 2014).

Methyl 2-(4-butyryl-5-hydroxy-2-methoxyphenoxy)acetate (4c) White solid (95%). *Rf* 0.53 (hexane/EtOAc 7:3); mp 121–122 °C (Lit. 122–123 °C, Mendieta et al. 2014).

Methyl 2-(2-chloro-5-hydroxy-4-propionylphenoxy)acetate (4d) White solid (74%). *Rf* 0.42 (hexane/EtOAc, 8:2); mp 142–143 °C. IR (KBr) ν_{\max} : 3085, 2956, 1772, 1636, 1498, 1439, 1370, 1211, 1188, 1084, 827 cm^{-1} ; ^1H NMR (300 MHz, CDCl_3) δ : 1.22 (t, $J = 7.5$ Hz, 3H, CH_3 -3"), 2.95 (q, $J = 7.5$ Hz, 2H, CH_2 -2"), 3.83 (s, 3H, OCH_3), 4.75 (s, 2H, CH_2 -2), 6.33 (s, 1H, H-6'), 7.77 (s, 1H, H-3'), 12.70 (s, 1H, OH); ^{13}C NMR (75 MHz, CDCl_3) δ : 8.1 (CH_3 -3"), 31.3 (CH_2 -2"), 52.6 (OCH_3), 65.5 (CH_2 -2), 101.6 (C-6'), 113.2

(C-2'), 114.0 (C-4'), 131.1 (C-3'), 158.8 (C-1'), 163.2 (C-5'), 167.7 (CO-1), 204.9 (CO-1''); MS (70 eV) m/z 274 ($M^+ + 2$, 12), 272 (M^+ , 36), 245 (36), 243 (100), 185 (13), 183 (15), 171 (15). HRMS (70 eV) Calculated for $C_{12}H_{13}ClO_5$: 272.0451. Found: 272.0457.

Methyl 2-(4-butyl-2-chloro-5-hydroxyphenoxy)acetate (4e)

White solid (80%). *Rf* 0.62 (hexane/EtOAc, 7:3); mp 118–119 °C. IR (KBr) ν_{\max} : 3425, 2966, 1771, 1632, 1494, 1371, 1208, 1085, 819 cm^{-1} ; 1H NMR (500 MHz, $CDCl_3$) δ : 1.02 (t, $J = 7.5$ Hz, 3H, CH_3-4''), 1.76 (sext, $J = 7.5$ Hz, 2H, CH_2-3''), 2.88 (t, $J = 7.5$ Hz, 2H, CH_2-2''), 3.82 (s, 3H, CO_2CH_3), 4.75 (s, 2H, CH_2-2), 6.34 (s, 1H, H-6'), 7.76 (s, 1H, H-3'), 12.74 (s, 1H, OH); ^{13}C NMR (125 MHz, $CDCl_3$) δ : 13.8 (CH_3-4''), 17.9 (CH_2-3''), 40.0 (CH_2-2''), 52.5 (CO_2CH_3), 65.5 (CH_2-2), 101.7 (C-6'), 113.3 (C-2'), 114.3 (C-4'), 131.3 (C-3'), 158.9 (C-1'), 163.5 (C-5'), 167.7 (CO_2CH_3-1), 204.6 (CO-1''). HRMS (70 eV) Calculated for $C_{13}H_{15}ClO_5$: 286.0608. Found: 286.0619.

2-(4-Acetyl-5-hydroxy-2-methoxyphenoxy)-1-(4-chlorophenyl)ethan-1-one (5a) White solid (83%). *Rf* 0.31 (hexane/EtOAc, 7:3); mp 148–149 °C. IR (KBr) ν_{\max} : 3397, 3087, 2938, 1710, 1629, 1589, 1510, 1402, 1373, 1334, 1266, 1232, 1202, 1090, 980, 837, 803 cm^{-1} ; 1H NMR (500 MHz, $CDCl_3$) δ : 2.56 (s, 3H, CH_3-1'''), 3.89 (s, 3H, OCH_3), 5.36 (s, 2H, CH_2-2), 6.30 (s, 1H, H-6''), 7.12 (s, 1H, H-3''), 7.46–7.50 (m, 2H, H-3'), 7.91–7.95 (m, 2H, H-2'), 12.50 (s, 1H, OH); ^{13}C NMR (125 MHz, $CDCl_3$) δ : 26.4 (CH_3-2'''), 57.0 (OCH_3), 70.8 (OCH_2-2), 101.8 (C-6''), 112.7 (C-4''), 113.0 (C-3''), 129.3 (C-3'), 129.4 (C-2'), 132.4 (C-1'), 140.7 (C-4'), 142.0 (C-2''), 154.9 (C-1''), 159.5 (C-5''), 191.6 (CO-1), 202.2 (CO-1'''); MS (70 eV) m/z 336 ($M^+ + 2$, 23), 334 (M^+ , 68), 195 (14), 167 (16), 141 (38), 140 (48), 139 (100). HRMS (70 eV) Calculated for $C_{17}H_{15}ClO_5$: 334.0608. Found: 334.0613.

1-(4-(2-(4-Chlorophenyl)-2-oxoethoxy)-2-hydroxy-5-methoxyphenyl)propan-1-one (5b) White solid (88%). *Rf* 0.42 (hexane/EtOAc, 7:3); mp 130–131 °C. IR (KBr) ν_{\max} : 3401, 3098, 2945, 1713, 1634, 1616, 1588, 1505, 1394, 1253, 1223, 1162, 1088, 979, 819 cm^{-1} ; 1H NMR (500 MHz, $CDCl_3$) δ : 1.23 (t, $J = 7.3$ Hz, 3H, CH_3-3), 2.94 (q, $J = 7.3$ Hz, 2H, CH_2-2), 3.88 (s, 3H, OCH_3), 5.36 (s, 2H, CH_2-1''), 6.30 (s, 1H, H-3'), 7.16 (s, 1H, H-6'), 7.46–7.50 (m, 2H, H-3''), 7.90–7.95 (m, 2H, H-2''), 12.59 (s, 1H, OH); ^{13}C NMR (125 MHz, $CDCl_3$) δ : 8.3 (CH_3-3), 31.4 (CH_2-2), 57.0 (OCH_3), 70.7 (CH_2-1''), 101.9 (C-3'), 112.1 (C-1'), 112.2 (C-6'), 129.3 (C-3''), 129.4 (C-2''), 132.4 (C-1''), 140.6 (C-4''), 142.0 (C-5'), 154.6 (C-4'), 159.4 (C-2'), 191.6 (CO-2''), 204.9 (CO-1); MS (70 eV) m/z 350 ($M^+ + 2$, 37), 348 (M^+ , 99), 321 (33), 319 (100), 167 (37), 153 (22), 141 (35), 139 (94), 125 (31). HRMS (70 eV) Calculated for $C_{18}H_{17}ClO_5$: 348.0764. Found: 348.0771.

1-(4-(2-(4-Chlorophenyl)-2-oxoethoxy)-2-hydroxy-5-methoxyphenyl)butan-1-one (5c) White solid (70%). *Rf* 0.48 (hexane/EtOAc, 7:3); mp 152–153 °C. IR (KBr) ν_{\max} : 3384, 3092, 2967, 1702, 1616, 1507, 1451, 1388, 1329, 1254, 1202, 1158, 1093, 1021, 965, 855, 826, 779 cm^{-1} ; 1H NMR (500 MHz, $CDCl_3$) δ : 1.03 (t, $J = 7.5$ Hz, 3H, CH_3-4), 1.77 (sext, $J = 7.5$ Hz, 2H, CH_2-3), 2.87 (t, $J = 7.5$ Hz, 2H, CH_2-2), 3.89 (s, 3H, OCH_3), 5.36 (s, 2H, OCH_2 , H-1''), 6.30 (s, 1H, H-3'), 7.17 (s, 1H, H-6'), 7.46–7.50 (m, 2H, H-3''), 7.91–7.96 (m, 2H, H-2''), 12.65 (s, 1H, OH); ^{13}C NMR (125 MHz, $CDCl_3$) δ : 13.9 (CH_3-4), 17.9 (CH_2-3), 40.0 (CH_2-2), 57.1 (OCH_3), 70.8 (CH_2-1''), 102.0 (C-3'), 112.4 (C-1'), 112.5 (C-6'), 129.3 (C-3''), 129.5 (C-2''), 132.5 (C-1''), 140.7 (C-4''), 142.0 (C-5'), 154.7 (C-4'), 159.7 (C-2'), 191.6 (CO-2''), 204.5 (CO-1); MS (70 eV) m/z 364 ($M^+ + 2$, 38), 362 (M^+ , 100), 321 (31), 319 (99), 167 (33), 153 (20), 141 (22), 139 (74), 125 (30). HRMS (70 eV) Calculated for $C_{19}H_{19}ClO_5$: 362.0921. Found: 362.0924.

1-(4-Chlorophenyl)-2-(5-hydroxy-2-methoxy-4-(2-phenylacetyl)phenoxy)ethan-1-one (5d) White solid (80%). *Rf* 0.65 (hexane/EtOAc, 6:4); mp 151–152 °C. IR (KBr) ν_{\max} : 3449, 3068, 2932, 1700, 1631, 1590, 1510, 1400, 1358, 1263, 1233, 1159, 974, 825 cm^{-1} ; 1H NMR (500 MHz, $CDCl_3$) δ : 3.83 (s, 3H, OCH_3), 4.21 (s, 2H, CH_2-2'''), 5.35 (s, 2H, OCH_2), 6.29 (s, 1H, H-6''), 7.22 (s, 1H, H-3''), 7.26–7.29 (m, 3H, H-2^{IV}, H-4^{IV}), 7.32–7.37 (m, 2H, H-3^{IV}), 7.46–7.50 (m, 2H, H-3'), 7.90–7.94 (m, 2H, H-2'), 12.47 (s, 1H, OH); ^{13}C NMR (125 MHz, $CDCl_3$) δ : 45.5 (CH_2-2'''), 56.8 (OCH_3), 70.8 (OCH_2), 101.9 (C-6''), 111.9 (C-4''), 112.7 (C-3''), 127.2 (C-4^{IV}), 128.8 (C-3^{IV}), 129.2 (C-2^{IV}), 129.3 (C-3'), 129.4 (C-2'), 132.4 (C-1'), 134.3 (C-1^{IV}), 140.7 (C-4'), 142.0 (C-2''), 154.9 (C-1''), 160.1 (C-5''), 191.5 (CO-1), 201.6 (CO-1'''); MS (70 eV) m/z 410 (M^+ , 22), 321 (35), 319 (100), 195 (21), 167 (59), 153 (43), 139 (35), 125 (37), 111 (22). HRMS (70 eV) Calculated for $C_{23}H_{19}ClO_5$: 410.0921. Found: 410.0941.

1-(5-Chloro-4-(2-(4-chlorophenyl)-2-oxoethoxy)-2-hydroxyphenyl)propan-1-one (5e) White solid (80%). *Rf* 0.65 (hexane/EtOAc, 8:2); mp 166–168 °C. IR (KBr) ν_{\max} : 3373, 3105, 2925, 1698, 1632, 1589, 1491, 1374, 1236, 1216, 1190, 1093, 973, 824 cm^{-1} ; 1H NMR (300 MHz, $DMSO-d_6$) δ : 1.12 (t, $J = 7.2$ Hz, 3H, CH_3-3), 2.90 (q, $J = 7.2$ Hz, 2H, CH_2-2), 5.53 (s, 2H, OCH_2), 6.49 (s, 1H, H-3'), 7.38–7.46 (m, 2H, H-3''), 7.75 (s, 1H, H-6'), 7.90–8.15 (m, 2H, H-2''), 12.52 (s, 1H, OH); ^{13}C NMR (75 MHz, $DMSO-d_6$) δ : 7.7 (CH_3-3), 30.8 (CH_2-2), 70.7 (OCH_2), 101.8 (C-3'), 112.3 (C-5'), 113.3 (C-1'), 128.6 (C-3''), 129.3 (C-2''), 130.6 (C-6'), 132.0 (C-1''), 139.6 (C-4''), 158.6 (C-4'), 162.6 (C-2'), 191.3 (CO-2''), 204.4 (CO-1); MS (70 eV) m/z 354 ($M^+ + 2$, 8), 352 (M^+ , 12), 317 (34), 141 (33), 139 (100), 125 (16). HRMS (70 eV) Calculated for $C_{17}H_{14}Cl_2O_4$: 352.0269. Found: 352.0271.

Methyl (E)-2-(4-(3-(dimethylamino)acryloyl)-5-hydroxy-2-methoxyphenoxy)acetate (E-12). Methyl (Z)-2-(4-(3-(dimethylamino)acryloyl)-5-hydroxy-2-methoxyphenoxy)acetate (Z-12). **Methyl 2-((6-methoxy-4-oxo-4H-chromen-7-yl)oxy)acetate (13)** A mixture of the compound **4a** (1.0 mol equiv.) with dimethylformamide dimethyl acetal (DMFDMA, 1.5 mol equiv.) was refluxed at 120 °C for 12 h (Correa et al. 2008; Labarrios et al. 2014). The reaction was cooled, filtered, and concentrated over vacuum. The residue was purified by flash chromatography to give a mixture of enaminones (E/Z)-**12** (72:28) as white solid (26%); *R*_f 0.22 (hexane/EtOAc, 1:2); mp 201–204 °C; and chromone **13** as white solid (44%); *R*_f 0.54 (EtOAc); mp 158–159 °C. **Data for (E)-12:** IR (KBr) ν_{\max} : 3462, 2952, 1743, 1629, 1533, 1501, 1434, 1379, 1292, 1249, 1230, 1156, 1112, 905, 843, 775 cm⁻¹; ¹H NMR (500 MHz, CDCl₃) δ : 2.98 (br, 3H, N(CH₃)), 3.18 (br, 3H, N(CH₃)), 3.80 (s, 3H, OCH₃-1), 3.88 (s, 3H, OCH₃-2'), 4.71 (s, 2H, CH₂, H-2), 5.61 (d, *J* = 12.0 Hz, 1H, H-2''), 6.31 (s, 1H, H-6'), 7.16 (s, 1H, H-3'). Signals attributed to the minor isomer (Z)-**12**: 3.83 (s, OCH₃), 3.98 (s, OCH₃), 4.80 (s, 2H, H-2), 6.30 (d, *J* = 6.0 Hz, 1H, H-2''), 6.78 (s, H-6'), 7.58 (s, H-3'), 7.79 (d, *J* = 6.0 Hz, 1H, H-3). ¹³C NMR (125 MHz, CDCl₃) δ : 37.4 (NCH₃), 45.2 (NCH₃), 52.3 (OCH₃-1), 57.5 (OCH₃-2'), 65.4 (C-2), 89.7 (C-2''), 102.0 (C-6'), 112.4 (C-3'), 112.9 (C-4'), 141.3 (C-2'), 153.0 (C-1'), 154.3 (C-3''), 159.7 (C-5'), 168.4 (CO-1), 190.2 (CO-1''). Signals attributed to the minor isomer (Z)-**12**: 52.5, 56.4, 66.0, 101.5, 105.2, 112.4, 119.3, 147.8, 152.3, 154.6, 168.1. HRMS (70 eV) Calculated for C₁₅H₁₉O₆: 309.1212. Found: 309.1220. **Data for 13:** IR (KBr) ν_{\max} : 2926, 1743, 1649, 1505, 1468, 1429, 1301, 1229, 1205, 1088, 842, 818 cm⁻¹; ¹H NMR (500 MHz, CDCl₃) δ : 3.83 (s, 3H, OCH₃-1), 3.98 (s, 3H, OCH₃-6'), 4.80 (s, 2H, CH₂-2), 6.30 (d, *J* = 6.0 Hz, 1H, H-3'), 6.78 (s, 1H, H-8'), 7.58 (s, 1H, H-5'), 7.79 (d, *J* = 6.0 Hz, 1H, H-2'); ¹³C NMR (125 MHz, CDCl₃) δ : 52.5 (OCH₃-1), 56.4 (OCH₃-6'), 66.0 (C-2), 101.5 (C-8'), 105.3 (C-5'), 112.4 (C-3), 119.4 (C-4a), 147.9 (C-6'), 152.0 (C-8a), 152.4 (C-7'), 154.6 (C-2'), 168.1 (CO-1), 176.6 (CO-4'); HRMS (70 eV) Calculated for C₁₃H₁₂O₆: 264.0634. Found: 264.0645.

General procedure for the synthesis of chromonyl enaminones 1–2 and 3-alkyl chromones 3

A mixture of the corresponding acyl phenol **6** or aryloxycarbonyl compound **4–5** (1.0 mol equiv.) with DMFDMA (3.0 mol equiv.) was refluxed at 120 °C for 48 h (Correa et al. 2008; Labarrios et al. 2014). The reaction was cooled, filtered, and concentrated over vacuum. The residue was purified by flash chromatography to give the respective chromones **1–3**.

Methyl (Z)-3-(dimethylamino)-2-((6-methoxy-4-oxo-4H-chromen-7-yl)oxy)acrylate (1a) Yellow solid (48%). *R*_f 0.42 (EtOAc); mp 181–183 °C. IR (KBr) ν_{\max} : 2925, 1694, 1632, 1433, 1299, 1205, 1115, 1088, 872, 764 cm⁻¹; ¹H NMR (300 MHz, CDCl₃) δ : 2.95 (s, 6H, N(CH₃)₂), 3.61 (s, 3H, CO₂CH₃), 3.96 (s, 3H, OCH₃), 6.27 (d, *J* = 6.0 Hz, 1H, H-3'), 6.90 (s, 1H, H-8'), 7.21 (s, 1H, H-3), 7.56 (s, 1H, H-5'), 7.77 (d, *J* = 6.0 Hz, 1H, H-2'); ¹³C NMR (75 MHz, CDCl₃) δ : 41.8 (N(CH₃)₂), 51.3 (CO₂CH₃), 56.4 (OCH₃), 102.6 (C-8'), 105.2 (C-5'), 112.2 (C-3'), 114.2 (C-2), 119.2 (C-4a'), 139.7 (C-3), 147.4 (C-6'), 152.3 (C-8a'), 154.2 (C-7'), 154.6 (C-2'), 165.5 (CO₂Me), 176.8 (CO-4'); MS (70 eV) *m/z* 319 (M⁺, 7), 274 (47), 260 (100), 232 (27), 203 (64), 189 (47), 160 (38), 144 (61), 134 (26), 116 (46), 84 (41). HRMS (70 eV) Calculated for C₁₆H₁₇NO₆: 319.1056. Found: 319.1064.

Methyl (Z)-3-(dimethylamino)-2-((6-methoxy-3-methyl-4-oxo-4H-chromen-7-yl)oxy)acrylate (1b) Yellow solid (65%). *R*_f 0.48 (EtOAc); mp 190–191 °C. IR (KBr) ν_{\max} : 2920, 1674, 1638, 1605, 1507, 1475, 1437, 1270, 1224, 1160, 1060, 864, 821, 773 cm⁻¹; ¹H NMR (300 MHz, CDCl₃) δ : 2.02 (d, *J* = 1.2 Hz, 3H, CH₃-C3'), 2.98 (s, 6H, N(CH₃)₂), 3.64 (s, 3H, CO₂CH₃), 3.99 (s, 3H, OCH₃), 6.89 (s, 1H, H-8'), 7.23 (s, 1H, H-3), 7.61 (s, 1H, H-5'), 7.74 (q, *J* = 1.2 Hz, 1H, H-2'); ¹³C NMR (75 MHz, CDCl₃) δ : 11.2 (CH₃-C3'), 41.8 (N(CH₃)₂), 51.2 (CO₂CH₃), 56.3 (OCH₃), 102.4 (C-8'), 105.1 (C-5'), 114.3 (C-2), 117.9 (C-4a'), 119.8 (C-3'), 139.7 (C-3), 147.2 (C-6'), 151.1 (C-2'), 152.4 (C-8a'), 153.8 (C-7'), 165.8 (CO₂Me), 177.4 (CO-4'); MS (70 eV) *m/z* 333 (M⁺, 22), 274 (100), 246 (7), 217 (27), 203 (7). HRMS (70 eV) Calculated for C₁₇H₁₉NO₆: 333.1212. Found: 333.1206.

Methyl (Z)-3-(dimethylamino)-2-((3-ethyl-6-methoxy-4-oxo-4H-chromen-7-yl)oxy)acrylate (1c) White solid (48%). *R*_f 0.57 (EtOAc); mp 138–139 °C. IR (KBr) ν_{\max} : 2936, 1690, 1621, 1469, 1433, 1301, 1267, 1226, 1181, 1207, 1086, 878, 760 cm⁻¹; ¹H NMR (500 MHz, CDCl₃) δ : 1.19 (t, *J* = 7.0 Hz, 3H, CH₃CH₂), 2.45 (q, *J* = 7.0 Hz, 2H, CH₃CH₂), 2.97 (s, 6H, N(CH₃)₂), 3.64 (s, 3H, CO₂CH₃), 4.00 (s, 3H, OCH₃), 6.88 (s, 1H, H-8'), 7.22 (s, 1H, H-3), 7.61 (s, 1H, H-5'), 7.68 (s, 1H, H-2'); ¹³C NMR (125 MHz, CDCl₃) δ : 13.0 (CH₃CH₂), 19.1 (CH₃CH₂), 42.0 (N(CH₃)₂), 51.3 (CO₂CH₃), 56.4 (OCH₃), 102.5 (C-8'), 105.4 (C-5'), 114.5 (C-2), 118.3 (C-4a'), 125.3 (C-3'), 139.7 (C-3), 147.2 (C-6'), 150.9 (C-2'), 152.3 (C-8a'), 154.0 (C-7'), 165.7 (CO₂Me), 176.9 (CO-4'); MS (70 eV) *m/z* 347 (M⁺, 33), 288 (100), 260 (11), 231 (24), 217 (11). HRMS (70 eV) Calculated for C₁₈H₂₁NO₆: 347.1369. Found: 347.1377.

Methyl (Z)-2-((6-chloro-3-methyl-4-oxo-4H-chromen-7-yl)oxy)-3-(dimethylamino)acrylate (1d) 6-Chloro-7-methoxy-3-methyl-4H-chromen-4-one (**14a**): **1d**: White solid

(91%); *Rf* 0.42 (hexane/EtOAc, 1:2); mp 205–207 °C. **14a**: White solid (9%); *Rf* 0.65 (hexane/EtOAc, 6:4); mp 201–203 °C. **Data for 1d**: IR (KBr) ν_{\max} : 2946, 1699, 1635, 1605, 1440, 1308, 1255, 1217, 1182, 1167, 1084, 904, 761, 701 cm^{-1} ; ^1H NMR (300 MHz, CDCl_3) δ : 2.00 (d, $J = 0.9$ Hz, 3H, CH_3), 3.00 (s, 6H, $\text{N}(\text{CH}_3)_2$), 3.66 (s, 3H, CO_2CH_3), 6.91 (s, 1H, H-8'), 7.24 (s, 1H, H-3), 7.73 (br s, 1H, H-2'), 8.24 (s, 1H, H-5'); ^{13}C NMR (75 MHz, CDCl_3) δ : 11.1 (CH_3), 42.5 ($\text{N}(\text{CH}_3)_2$), 51.3 (CO_2CH_3), 103.0 (C-8'), 114.3 (C-2), 118.6 (C-6'), 120.4 (C-4a), 120.5 (C-3'), 127.0 (C-5'), 139.8 (C-3), 151.4 (C-2'), 156.4 (C-8a'), 158.7 (C-7'), 165.2 (CO_2Me), 176.7 (CO-4'). HRMS (70 eV) Calculated for $\text{C}_{16}\text{H}_{16}\text{ClNO}_5$: 337.0717. Found: 337.0718. **Data for 14a**: IR (KBr) ν_{\max} : 2924, 1649, 1606, 1453, 1267, 1168, 1047, 1018, 892, 848, 774, 693 cm^{-1} ; ^1H NMR (300 MHz, CDCl_3) δ : 2.01 (d, $J = 1.2$ Hz, 3H, CH_3), 3.99 (s, 3H, CO_2CH_3), 6.85 (s, 1H, H-8), 7.73 (br s, 1H, H-2), 8.19 (s, 1H, H-5); ^{13}C NMR (75 MHz, CDCl_3) δ : 11.1 (CH_3), 56.6 (OCH_3), 100.0 (C-8), 117.6 (C-6), 120.7 (C-3), 120.9 (C-4a), 126.5 (C-5), 151.3 (C-2), 156.6 (C-8a), 158.8 (C-7), 176.6 (CO-4). Anal. calcd for $\text{C}_{11}\text{H}_9\text{ClO}_3$: C, 58.81; H, 4.04. Found: C, 60.37; H, 4.67. HRMS (70 eV) Calculated for $\text{C}_{11}\text{H}_9\text{ClO}_3$: 224.0240. Found: 224.0239.

Methyl (Z)-2-((6-Chloro-3-ethyl-4-oxo-4H-chromen-7-yl)oxy)-3-(dimethylamino)acrylate (1e) 6-Chloro-3-ethyl-7-methoxy-4H-chromen-4-one (**14b**): **1e**: White solid (71%); *Rf* 0.37 (hexane/EtOAc, 1:1); mp 147–148 °C. **14b**: White solid (11%); *Rf* 0.71 (hexane/EtOAc, 1:1); mp 160–161 °C. **Data for 1e**: IR (KBr) ν_{\max} : 2946, 1699, 1639, 1605, 1467, 1439, 1354, 1303, 1254, 1218, 1183, 1122, 1085, 759, 694 cm^{-1} ; ^1H NMR (500 MHz, CDCl_3) δ : 1.18 (t, $J = 7.5$ Hz, 3H, CH_3CH_2), 2.48 (br q, $J = 7.5$ Hz, 2H, CH_3CH_2), 2.99 (s, 6H, $\text{N}(\text{CH}_3)_2$), 3.66 (s, 3H, CO_2CH_3), 6.90 (s, 1H, H-8'), 7.23 (s, 1H, H-3), 7.67 (br s, 1H, H-2'), 8.24 (s, 1H, H-5'); ^{13}C NMR (125 MHz, CDCl_3) δ : 12.9 (CH_3CH_2), 19.0 (CH_3CH_2), 42.5 ($\text{N}(\text{CH}_3)_2$), 51.3 (CO_2CH_3), 103.0 (C-8'), 114.5 (C-2), 119.0 (C-6'), 120.5 (C-4a'), 126.0 (C-3'), 127.1 (C-5'), 139.7 (C-3), 151.3 (C-2'), 156.3 (C-8a'), 158.8 (C-7'), 165.2 (CO_2Me), 176.2 (CO-4'). HRMS (70 eV) Calculated for $\text{C}_{17}\text{H}_{18}\text{NClO}_5$: 351.0873. Found: 351.0870. **Data for 14b**: IR (KBr) ν_{\max} : 2925, 1642, 1611, 1441, 1298, 1261, 1228, 1038, 894, 831 cm^{-1} ; ^1H NMR (500 MHz, CDCl_3) δ : 1.19 (t, $J = 7.5$ Hz, 3H, CH_3CH_2), 2.48 (br q, $J = 7.5$ Hz, 2H, CH_3CH_2), 3.98 (s, 3H, OCH_3), 6.85 (s, 1H, H-8), 7.68 (s, 1H, H-2), 8.19 (s, 1H, H-5); ^{13}C NMR (125 MHz, CDCl_3) δ : 12.8 (CH_3CH_2), 19.0 (CH_3CH_2), 56.6 (OCH_3), 100.0 (C-8), 118.0 (C-6), 121.0 (C-4a), 126.1 (C-3), 126.7 (C-5), 151.1 (C-2), 156.5 (C-8a), 158.8 (C-7), 176.2 (CO-4). HRMS (70 eV) Calculated for $\text{C}_{12}\text{H}_{11}\text{ClO}_3$: 238.0397. Found: 238.0394.

(Z)-7-((3-(4-chlorophenyl)-1-(dimethylamino)-3-oxoprop-1-en-2-yl)oxy)-6-methoxy-4-oxo-4H-chromene-3-carbaldehyde (2a) Yellow solid (82%). *Rf* 0.37 (EtOAc); mp 232–233 °C; IR (KBr) ν_{\max} : 2926, 1631, 1586, 1545, 1493, 1436, 1374, 1293, 1226, 1156, 1114, 960, 906, 845, 778 cm^{-1} ; ^1H NMR (300 MHz, CDCl_3) δ : 3.08 (s, 6H, $\text{N}(\text{CH}_3)_2$), 4.02 (s, 3H, OCH_3), 6.95 (s, 1H, H-8), 7.15 (br s, 1H, H-1'), 7.28–7.40 (m, 2H, H-3''), 7.56–7.67 (m, 2H, H-2''), 7.63 (s, 1H, H-5), 8.45 (s, 1H, H-2), 10.36 (s, 1H, CHO); ^{13}C NMR (75 MHz, CDCl_3) δ : 41.7 ($\text{N}(\text{CH}_3)_2$), 56.5 (OCH_3), 103.1 (C-8'), 105.6 (C-5'), 119.52 (C-3), 119.53 (C-4a), 125.9 (C-2'), 128.3 (C-3''), 129.7 (C-2''), 136.6 (C-4''), 137.2 (C-1''), 144.7 (C-1'), 148.2 (C-6), 151.8 (C-8a), 153.9 (C-7), 159.8 (C-2), 175.0 (CO-4), 186.0 (CO-3'), 188.9 (CHO); MS (70 eV) m/z 427 (M^+ , 22), 288 (100), 260 (23), 231 (22), 218 (48), 191 (26), 139 (20). Anal. calcd for $\text{C}_{22}\text{H}_{18}\text{ClNO}_6$: C, 61.76; H, 4.24; N, 3.27. Found: C, 61.73; H, 4.27; N, 3.27.

(Z)-7-((3-(4-chlorophenyl)-1-(dimethylamino)-3-oxoprop-1-en-2-yl)oxy)-6-methoxy-3-methyl-4H-chromen-4-one (2b) Yellow solid (73%). *Rf* 0.25 (hexane/EtOAc 1:2). mp 239–241 °C; IR (KBr) ν_{\max} : 2928, 1637, 1606, 1580, 1556, 1481, 1327, 1269, 1206, 1176, 1123, 937, 841, 755 cm^{-1} ; ^1H NMR (500 MHz, CDCl_3) δ : 1.99 (d, $J = 1.0$ Hz, 3H, CH_3), 3.06 (s, 6H, $\text{N}(\text{CH}_3)_2$), 3.98 (s, 3H, OCH_3), 6.84 (s, 1H, H-8), 7.16 (br s, 1H, H-1'), 7.30 (br d, $J = 8.0$ Hz, 2H, H-3''), 7.56 (s, 1H, H-5), 7.62 (br d, $J = 8.0$ Hz, 2H, H-2''), 7.68 (br s, 1H, H-2); ^{13}C NMR (125 MHz, CDCl_3) δ : 11.2 (CH_3), 41.7 ($\text{N}(\text{CH}_3)_2$), 56.4 (OCH_3), 102.5 (C-8), 105.5 (C-5), 118.1 (C-4a), 119.9 (C-3), 126.2 (C-2'), 128.2 (C-3''), 129.8 (C-2''), 136.6 (C-4''), 137.4 (C-1''), 144.7 (C-1'), 147.2 (C-6), 151.1 (C-2), 152.4 (C-8a), 153.2 (C-7), 177.3 (CO-4), 186.5 (CO-3'); MS (70 eV) m/z 415 ($\text{M}^+ + 2$, 12), 413 (M^+ , 29), 383 (6), 274 (100), 246 (18), 217 (23), 204 (43) 191 (12), 139 (15), 111 (9). Anal. calcd for $\text{C}_{22}\text{H}_{20}\text{ClNO}_5$: C, 63.85; H, 4.87; N, 3.38. Found: C, 63.86; H, 4.88; N, 3.40.

(Z)-7-((3-(4-chlorophenyl)-1-(dimethylamino)-3-oxoprop-1-en-2-yl)oxy)-3-ethyl-6-methoxy-4H-chromen-4-one (2c) Yellow solid (94%). *Rf* 0.28 (hexane/EtOAc, 1:2); mp 176–177 °C. IR (KBr) ν_{\max} : 2963, 1640, 1578, 1487, 1432, 1329, 1269, 1209, 1120, 1056, 958, 919, 837, 754 cm^{-1} ; ^1H NMR (300 MHz, CDCl_3) δ : 1.17 (t, $J = 7.5$ Hz, 3H, CH_3CH_2), 2.47 (br q, $J = 7.5$ Hz, 2H, CH_3CH_2), 3.06 (s, 6H, $\text{N}(\text{CH}_3)_2$), 3.98 (s, 3H, OCH_3), 6.85 (s, 1H, H-8), 7.18 (br s, 1H, H-1'), 7.27–7.36 (m, 2H, H-3''), 7.57 (s, 1H, H-5), 7.60–7.70 (m, 2H, H-2''), 7.66 (br s, 1H, H-2); ^{13}C NMR (75 MHz, CDCl_3) δ : 12.9 (CH_3CH_2), 19.0 (CH_3CH_2), 41.7 ($\text{N}(\text{CH}_3)_2$), 56.2 (OCH_3), 102.3 (C-8), 105.4 (C-5), 118.2 (C-4a), 125.2 (C-3), 126.1 (C-2'), 128.1 (C-3''), 129.7 (C-2''), 136.4 (C-4''), 137.2 (C-1''), 144.7 (C-1'), 147.1 (C-6), 150.9 (C-2), 152.1 (C-8a), 153.1 (C-7), 176.8

(CO-4), 186.3 (CO-3'); MS (70 eV) m/z 429 ($M^+ + 2$, 9), 427 (M^+ , 28), 410 (5), 396 (4), 288 (100), 260 (16), 231 (21), 218 (35), 217 (20), 208 (9), 191 (10), 139 (12). Anal. calcd for $C_{23}H_{22}ClNO_5$: C, 64.56; H, 5.18; N, 3.27. Found: C, 64.56; H, 5.18; N, 3.29.

(Z)-7-((3-(4-chlorophenyl)-1-(dimethylamino)-3-oxoprop-1-en-2-yl)oxy)-6-methoxy-3-phenyl-4H-chromen-4-one (2d)

Yellow solid (67%). *Rf* 0.34 (hexane/EtOAc, 1:2); mp 205–206 °C. IR (KBr) ν_{\max} : 2925, 1639, 1579, 1488, 1468, 1430, 1326, 1267, 1210, 1123, 960, 827, 793, 748 cm^{-1} ; 1H NMR (300 MHz, $CDCl_3$) δ : 3.06 (s, 6H, $N(CH_3)_2$), 3.99 (s, 3H, OCH_3), 6.91 (s, 1H, H-8), 7.17 (br s, 1H, H-1''), 7.28–7.46 (m, 5H, H-3', H-4', H-3'''), 7.51–7.57 (m, 2H, H-2'), 7.61–7.70 (m, 3H, H-2'', H-5), 7.91 (s, 1H, H-2); ^{13}C NMR (75 MHz, $CDCl_3$) δ : 41.5 ($N(CH_3)_2$), 56.4 (OCH_3), 102.5 (C-8), 106.0 (C-5), 119.0 (C-4a), 124.6 (C-3), 126.1 (C-2''), 128.0 (C-4'), 128.2 (C-3'''), 128.4 (C-2'), 128.9 (C-3'), 129.8 (C-2'''), 132.0 (C-1'), 136.6 (C-4'''), 137.2 (C-1'''), 144.6 (C-1''), 147.5 (C-6), 151.8 (C-8a), 152.4 (C-2), 153.4 (C-7), 175.2 (CO-4), 186.3 (CO-3'); MS (70 eV) m/z 477 ($M^+ + 2$, 8), 475 (M^+ , 19), 458 (5), 444 (4), 336 (100), 308 (16), 279 (16), 266 (41), 139 (12). Anal. calcd for $C_{27}H_{22}ClNO_5$: C, 68.14; H, 4.66; N, 2.94. Found: C, 68.15; H, 4.66; N, 2.95.

(Z)-6-chloro-7-((3-(4-chlorophenyl)-1-(dimethylamino)-3-oxoprop-1-en-2-yl)oxy)-3-methyl-4H-chromen-4-one (2e)

6-Chloro-7-methoxy-3-methyl-4H-chromen-4-one (**14a**): **2a**: White solid (82%); *Rf* 0.22 (hexane/EtOAc, 6:4); mp 225–226 °C. **14a**: White solid (9%); *Rf* 0.65 (hexane/EtOAc, 6:4); mp 202–203 °C. **Data for 2e**: IR (KBr) ν_{\max} : 3056, 2924, 1640, 1602, 1443, 1327, 1258, 1219, 1171, 1122, 995, 937, 840 cm^{-1} ; 1H NMR (300 MHz, $CDCl_3$) δ : 1.98 (d, $J = 1.2$ Hz, 3H, CH_3), 3.08 (s, 6H, $N(CH_3)_2$), 6.86 (s, 1H, H-8), 7.23 (br s, 1H, H-1'), 7.29–7.40 (m, 2H, H-3''), 7.57–7.74 (m, 2H, H-2''), 7.68 (br s, 1H, H-2), 8.19 (s, 1H, H-5); ^{13}C NMR (75 MHz, $CDCl_3$) δ : 11.1 (CH_3), 41.7 ($N(CH_3)_2$), 102.9 (C-8), 118.7 (C-6), 120.4 (C-4a), 120.6 (C-3), 126.2 (C-2), 127.1 (C-5), 128.3 (C-3'''), 129.8 (C-2''), 136.8 (C-1''), 136.9 (C-4'''), 144.1 (C-1'), 151.4 (C-2), 156.3 (C-8a), 157.8 (C-7), 176.6 (CO-4), 186.1 (CO-3'). Anal. calcd for $C_{21}H_{17}NO_4Cl_2$: C, 60.30; H, 4.10; N, 3.35. Found: C, 60.31; H, 4.13; N, 3.33.

6,7-Dimethoxy-4-oxo-4H-chromene-3-carbaldehyde

(3a) (*E/Z*)-3-(Dimethylamino)-1-(2-hydroxy-4,5-dimethoxyphenyl)prop-2-en-1-one (**15**): **3a**: Yellow solid (67%); *Rf* 0.26 (hexane/EtOAc, 6:4); mp 211–212 °C (Lit. 226.0–226.5 °C, Nohara et al. 1974). (*E/Z*)-**15** (85:15): Yellow solid (23%); *Rf* 0.31 (hexane/EtOAc, 1:2); mp 155–158 °C (Lit. 157–158 °C, Chin et al. 2015). **Data for**

3a: IR (KBr) ν_{\max} : 3071, 1697, 1645, 1619, 1504, 1475, 1437, 1303, 1270, 1246, 1157, 1000, 780 cm^{-1} ; 1H NMR (500 MHz, $CDCl_3$) δ : 4.00 (s, 6H, $(OCH_3)_2$), 6.94 (s, 1H, H-8), 7.61 (s, 1H, H-5), 8.49 (s, 1H, H-2), 10.41 (s, 1H, CHO); ^{13}C NMR (125 MHz, $CDCl_3$) δ : 56.5 (OCH_3), 56.6 (OCH_3), 100.1 (C-8), 104.6 (C-5), 118.7 (C-4a), 119.8 (C-3), 148.6 (C-6), 152.3 (C-8a), 155.1 (C-7), 159.6 (C-2), 177.3 (CO-4), 189.0 (CHO); MS (70 eV) m/z 234 (M^+ , 3), 206 (100), 191 (51), 183 (12), 137 (16), 107 (20). HRMS (70 eV) Calculated for $C_{12}H_{10}O_5$: 234.0528. Found: 234.0528. **Data for (E)-15**: 1H NMR (500 MHz, $CDCl_3$) δ : 2.98 (br, 3H, $N(CH_3)$), 3.18 (br, 3H, $N(CH_3)$), 3.86 (s, 3H, OCH_3 -5'), 3.89 (s, 3H, OCH_3 -4'), 5.61 (d, $J = 12.5$ Hz, 1H, H-2), 6.45 (s, 1H, H-3'), 7.11 (s, 1H, H-6'), 7.85 (d, $J = 12.5$ Hz, 1H, H-3). Signals attributed to the minor isomer (*Z*)-**15**: 3.98 (s, OCH_3), 4.00 (s, OCH_3), 6.30 (d, $J = 6.0$ Hz, H-2), 6.87 (s, H-3'), 7.54 (s, H-6'), 7.80 (d, $J = 6.0$ Hz, H-3). ^{13}C NMR (125 MHz, $CDCl_3$) δ : 37.4 (NCH_3), 45.2 (NCH_3), 55.9 (OCH_3 -4'), 57.1 (OCH_3 -5'), 89.7 (C-2), 100.8 (C-3'), 111.1 (C-6'), 111.7 (C-1'), 141.2 (C-5'), 154.1 (C-3), 155.0 (C-4'), 160.1 (C-2'), 190.3 (CO). Signals attributed to the minor isomer (*Z*)-**15**: 99.3, 104.0, 112.3, 159.1. HRMS (70 eV) Calculated for $C_{13}H_{17}NO_4$: 251.1158. Found: 251.1156.

6,7-Dimethoxy-3-methyl-4H-chromen-4-one (3b)

White solid (96%). *Rf* 0.23 (hexane/EtOAc, 6:4); mp 151–152 °C. IR (KBr) ν_{\max} : 2956, 1640, 1602, 1508, 1477, 1430, 1325, 1268, 1228, 1177, 1026, 770 cm^{-1} ; 1H NMR (500 MHz, $CDCl_3$) δ : 2.03 (s, 1H, CH_3), 3.97 (s, 3H, OCH_3), 3.98 (s, 3H, OCH_3), 6.83 (s, 1H, H-8), 7.56 (s, 1H, H-5), 7.74 (br s, 1H, H-2); ^{13}C RMN (125 MHz, $CDCl_3$) δ : 11.2 (CH_3), 56.2 (OCH_3), 56.3 (OCH_3), 99.5 (C-8), 104.3 (C-5), 117.0 (C-4a), 120.0 (C-3), 147.4 (C-6), 151.0 (C-2), 152.7 (C-8a), 154.1 (C-7), 177.4 (CO); MS (70 eV) m/z 220 (M^+ , 100), 219 (33), 205 (26), 191 (17), 177 (30), 174 (36), 161 (16), 149 (17), 137 (12). HRMS (70 eV) Calculated for: $C_{12}H_{12}O_4$. 220.0736. Found: 220.0744.

3-Ethyl-6,7-dimethoxy-4H-chromen-4-one (3c)

White solid (98%). *Rf* 0.38 (hexane/EtOAc, 6:4); mp 117–118 °C. IR (KBr) ν_{\max} : 2966, 1641, 1605, 1506, 1473, 1430, 1299, 1267, 1244, 1224, 1194, 1145, 1008, 820, 755 cm^{-1} ; 1H NMR (500 MHz, $CDCl_3$) δ : 1.20 (t, $J = 7.5$ Hz, 3H, CH_3CH_2), 2.50 (q, $J = 7.5$ Hz, 2H, CH_3CH_2), 3.96 (s, 3H, OCH_3), 3.97 (s, 3H, OCH_3), 6.82 (s, 1H, H-8), 7.55 (s, 1H, H-5), 7.70 (s, 1H, H-2); ^{13}C NMR (125 MHz, $CDCl_3$) δ : 12.9 (CH_3CH_2), 19.1 (CH_3CH_2), 56.2 (OCH_3), 56.3 (OCH_3), 99.4 (C-8), 104.3 (C-5), 117.2 (C-4a), 125.3 (C-3), 147.3 (C-6), 150.8 (C-2), 152.5 (C-8a), 154.0 (C-7), 176.8 (CO); MS (70 eV) m/z 234 (M^+ , 100), 233 (83), 219 (25), 191 (21), 175 (14). HRMS (70 eV) Calculated for $C_{13}H_{14}O_4$: 234.0892. Found: 234.0889.

6,7-Dimethoxy-3-propyl-4H-chromen-4-one (3d) White solid (99%). *Rf* 0.44 (hexane/EtOAc, 6:4); mp 107–108 °C. IR (KBr) ν_{\max} : 2956, 1641, 1607, 1505, 1474, 1432, 1324, 1269, 1225, 1149, 1080, 1002, 821, 767 cm^{-1} ; ^1H NMR (500 MHz, CDCl_3) δ : 0.97 (t, $J = 7.5$ Hz, 3H, $\text{CH}_3\text{CH}_2\text{CH}_2$), 1.62 (sext, $J = 7.5$ Hz, 2H, $\text{CH}_3\text{CH}_2\text{CH}_2$), 2.44 (t, $J = 7.5$ Hz, 2H, $\text{CH}_3\text{CH}_2\text{CH}_2$), 3.96 (s, 3H, OCH_3), 3.97 (s, 3H, OCH_3), 6.82 (s, 1H, H-8), 7.55 (s, 1H, H-5), 7.69 (s, 1H, H-2); ^{13}C NMR (125 MHz, CDCl_3) δ : 13.7 ($\text{CH}_3\text{CH}_2\text{CH}_2$), 21.5 ($\text{CH}_3\text{CH}_2\text{CH}_2$), 27.8 ($\text{CH}_3\text{CH}_2\text{CH}_2$), 56.1 (OCH_3), 56.2 (OCH_3), 99.4 (C-8), 104.4 (C-5), 117.3 (C-4a), 123.7 (C-3), 147.3 (C-6), 151.2 (C-2), 152.5 (C-8a), 154.1 (C-7), 176.9 (CO); MS (70 eV) m/z 248 (M^+ , 70), 247 (38), 233 (84), 220 (100), 205 (19), 191 (19), 174 (26). HRMS (70 eV) Calculated for $\text{C}_{14}\text{H}_{16}\text{O}_4$: 248.1049. Found: 248.1040.

3-Isopropyl-6,7-dimethoxy-4H-chromen-4-one (3e) White solid (98%). *Rf* 0.50 (hexane/EtOAc, 6:4); mp 92–93 °C. IR (KBr) ν_{\max} : 2957, 1632, 1602, 1508, 1479, 1456, 1271, 1225, 1065, 822, 765 cm^{-1} ; ^1H NMR (500 MHz, CDCl_3) δ : 1.23 (d, $J = 7.5$ Hz, 6H, $(\text{CH}_3)_2\text{CH}$), 3.16 (sept, $J = 7.5$ Hz, 1H, $(\text{CH}_3)_2\text{CH}$), 3.97 (s, 6H, $(\text{OCH}_3)_2$), 6.83 (s, 1H, H-8), 7.56 (s, 1H, H-5), 7.67 (s, 1H, H-2); ^{13}C NMR (125 MHz, CDCl_3) δ : 21.5 ($(\text{CH}_3)_2$), 25.0 ($(\text{CH}_3)_2\text{CH}$), 56.2 (OCH_3), 56.3 (OCH_3), 99.4 (C-8), 104.5 (C-5), 117.4 (C-4a), 129.5 (C-3), 147.3 (C-6), 150.5 (C-2), 152.3 (C-8a), 154.1 (C-7), 176.4 (CO); MS (70 eV) m/z 248 (M^+ , 77), 247 (43), 233 (100), 220 (91), 205 (14), 189 (16), 174 (15). HRMS (70 eV) Calculated for $\text{C}_{14}\text{H}_{16}\text{O}_4$: 248.1049. Found: 248.1041.

Single-crystal X-ray crystallography

Enaminone **1b** was obtained as colorless crystals by crystallization from EtOAc/ CH_2Cl_2 (9:1), which were mounted on glass fibers. Crystallographic measurements were performed on an Oxford XCalibur diffractometer with Mo $\text{K}\alpha$ radiation ($\lambda = 0.71073$ Å; graphite monochromator) at room temperature, with a CCD detector. Empirical (multi-scan) absorption corrections were applied. Unit cell parameters were obtained from a least-squares refinement and intensities were corrected for Lorentz and polarization effects. Hydrogen atoms were placed from an electron density map and their atomic coordinates refined. Unit weights were used in the refinement. After being solved with SHELXT (Sheldrick 2008, 2015), implemented in the WinGX suite (Farrugia 1999, 2012), and refined within WinGX using SHELXL (Sheldrick 2015). ORTEP diagram was made with ORTEP3 (Farrugia 1997, 2012). Data from **1b**: Formula: $\text{C}_{17}\text{H}_{19}\text{NO}_6$; molecular weight: 333.33; cryst. syst.: triclinic; space group: P-1; unit cell parameters: a , 6.2438 (3), b , 11.2551(5), c , 12.7475(7) (Å); α , 65.846(5)°, β , 84.544(4)°, γ , 89.373(4)°; temp. (K): 292(2); Z: 2; No. of reflections collected: 10497; No. of independent reflections:

5139; No. of observed reflections: 2935; data collection range: $3.147 < \theta < 32.412$ °; R : 0.0638; wR : 0.1374; GOF: 1.034. The authors have deposited the atomic coordinates for this structure with the Cambridge Crystallographic Data Centre (CCDC 1884808). The coordinates can be obtained, on request, from the Director Cambridge Crystallographic Data Centre, 12 Union Road, Cambridge, CB2 1EZ, UK.

Biological evaluation

Enzyme inhibition study

The determination of α -glucosidase inhibition was carried out according to a published method (Salehi et al. 2013), with some modifications. A solution of 20 μL α -glucosidase (0.5 unit/mL), 120 μL of 0.1 M phosphate buffer (pH 6.9) and 10 μL of the sample was prepared at various concentrations. The solution was incubated in 96-well plates at 37 °C for 15 min. Then the enzymatic reaction was initiated by adding 20 μL of 5 mM *p*-nitrophenyl- α -D-glucopyranoside solution in 0.1 M phosphate buffer (pH 6.9), followed by incubation of the mixture for another 15 min at 37 °C. The reaction was ended by adding 80 μL of 0.2 M sodium carbonate solution and then absorbance was read was recorded at 405 nm by a microplate reader (Epoch, Bio-Tek®). The reaction system without test compounds served as the control, and the system without α -glucosidase was as the blank for correcting the background absorbance. The percentage of α -glucosidase inhibition produced by the sample was calculated by using Eq. (1).

$$\% \text{ de inhibition} = \left(\frac{\text{Control absorbance} - \text{sample absorbance}}{\text{Control absorbance}} \right) \times 100 \quad (1)$$

DPPH radical scavenging assay

The scavenging of free radicals by the chromones was assessed with a DPPH assay as previously described (Cevallos-Casals and Cisneros-Zevallos 2003), with slight modifications. Concentrations were prepared of 10, 1.0, and 0.1 mM of each of the compounds, to which a solution of 2,2-diphenyl-1-picrylhydrazyl radical (DPPH) (133.33 μM) was added at a ratio of 1:3 (v/v). The mixture was incubated at 37 °C for 30 min and read at 517 nm. Antioxidant activity was expressed as the percentage of decrease of DPPH at 10 mM (%).

Antimicrobial activity

Compounds **1–3** were evaluated for their inhibition of two strains (ATCC 90028/ATCC 10231) and 20 clinical isolates of *Candida albicans*. The broth microdilution method was

utilized with resazurin as an indicator of cell viability (Sarker et al. 2007). For the incubations (at 30 °C), different concentrations of the test compounds (10–500 µg/mL, each with 5×10^5 CFU) were placed in each well of a 96-well plate containing PDB medium and resazurin to reach a final volume of 0.3 mL in quintuplicate ($n = 15$). Fluconazole was used as the reference (0.1–200 µg/mL). The absorbance was recorded at 545 nm after 12 h. The MIC value was considered as the initial concentration capable of avoiding any change of absorbance in the dose response curves. The inhibitory efficiency of each chromone was validated by ANOVA and the Tukey test ($p < 0.05$) on GraphPad Prism 7.0 software.

Docking studies

The proposed chemical structures (Scheme 1) were drawn in 2D format on ACD/ChemSketch 14.01 software (ACD/ChemSketch 2012). Subsequently, explicit hydrogen atoms were added to the molecule, and a geometric 3D pre-optimization was performed. The Z matrix of each molecule was created on the GaussView 5.0.9 package (Dennington et al. 2012). The molecules were submitted to a geometric and energetic optimization with semi-empirical molecular orbitals AM1 (Austin Model 1) on the GAUSSIAN 09W 9.5 program (Dennington et al. 2012). The results were converted to a.mol file with the GaussView graphical interface (Dennington et al. 2012) and then to pdb with Pymol (DeLano 2002), these being the input files for docking simulations.

The molecular docking studies were carried out on the AutoDock 4.2 program (Morris et al. 2009) using the α -glucosidase 3D structure located at Protein Data Base (PDB: 2ZE0). Polar hydrogen atoms and atomic partial charges were included by using the AutoDock Tools 1.5.6 program. To examine the electrostatic contribution of the ligand–receptor interaction, the Kollman partial charges were calculated (Morris et al. 2009). The analysis was

performed with blind docking, adjusting the grid box size to $60 \times 60 \times 60 \text{ \AA}$ with grid point spacing of 0.375 \AA^3 . The focus was CZ of Arg197 because it is a key residue that participates in the recognition process of other reported ligands (Jhon et al. 2015). All docking simulations were based on the Lamarckian genetic algorithm considering a randomized initial population of 100 individuals and a maximum number of energy evaluations of 1×10^7 . The atomic affinity maps were generated on the AutoGrid 4.0 program. The 3-D ligand–receptor complexes were visualized and analyzed on the AutoDock Tools program, taking into account the different interactions formed in each complex and selecting the complex with the lowest free energy values. This was the procedure for identifying the key residues involved in the process of molecular recognition of ligands by the receptor. The main criterion for choosing the best molecules was free energy (ΔG) because it determines the dissociation constant (K_d) or inhibitory constant (K_i) and the binding pose.

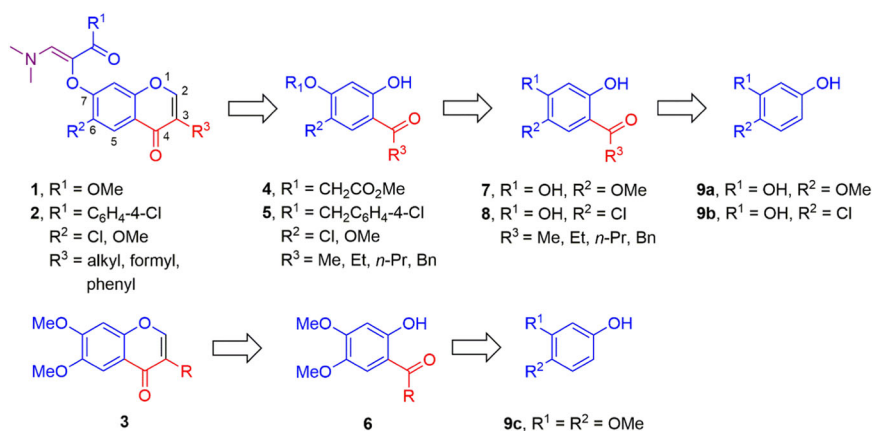
Results and discussion

Chemistry

Based on previously reported results from biological and docking studies using chromone inhibitors (Philip et al. 2017; Zhen et al. 2017; Wang et al. 2017, 2018; Jose et al. 2018; Soengas et al. 2016), we designed the target compound series 1–3. To each series, an alkyl chain or a phenyl group was added to the C-3 position of the pyrone ring. Considering the introduction of a tertiary amino group for compounds 1–2, an enaminoone scaffold was added at the C-7 position of the aromatic ring of the chromone. For compounds 3a–e, a methoxy group was incorporated at this position (Scheme 1).

Detailed procedures for the synthesis of 2-acyl phenols 6a and 6c (Mendieta et al. 2014), 6b (Musso et al. 2010), 6e

Scheme 1 Retrosynthesis of alkyl chromones derivatives 1–3



(Huls 1958), **8a** (Zoe et al. 2010), **8b** (Jha et al. 1981), **8d** (Goto et al. 2009), **9a** (Rao and Krupadanam 1994), and **9b** (Moore et al. 1934) have been described. Thus, the series of compounds **6–8** were prepared by acylation of phenols **9a–c** with the corresponding acyl chlorides **10a–e**, in the presence of boron trifluoride etherate ($\text{BF}_3 \cdot \text{OEt}_2$) at 80 °C for 3 h, to give 2-acyl phenols in high yields (Table 1). The ^1H NMR spectra of the acyl phenols **6–8** show a single signal for the hydroxyl group in the 12.65–12.75 ppm range. The ^{13}C NMR spectra display a signal at around 204 ppm, which is characteristic of the C-1 carbonyl group.

Subsequently, the series of compounds **7** and **8** were subjected to the *O*-alkylation reaction by employing α -bromoester (**11a**) or α -bromoacetophenone (**11b**) in the presence of potassium carbonate in acetone at reflux, obtaining the corresponding series of aryloxycarbonyl compounds **4–5** in high yields (Table 2). The ^1H NMR spectra of these two series show a single signal in the range of 4.63–5.53 ppm, which is attributed to the methylene protons of the oxyacetic group. In the ^{13}C NMR spectra, there is a signal at around 168 or 191 ppm assigned to the C-1 carbonyl group.

Ketones and esters containing an α -methylene group readily condense with DMFDMA to afford enaminones under solvent-free thermal conditions (Correa et al. 2008).

Initially, the aryloxyacetic ester **4a** was reacted with DMFDMA (1.5 mol equiv.) at 120 °C for 12 h. However, a mixture of enaminones *E/Z*-**12** (72:28) (26%) and chromone **13** (44%) were isolated as the main products (Scheme 2). Since the series of compounds **4** and **5** possess two activated methylene groups, the DMFDMA reagent had to be used in an excess (3.0 mol equiv.) at 120 °C for longer reaction times (48 h), resulting in the corresponding chromonyl enaminones **1a–e** and **2a–e** in moderate to good yields (Table 3). Unexpectedly, when the reaction was carried out with **4d–e** and **5e**, chromones **14a–b** were isolated as by-products in low yields. These were probably generated by breakage of the phenoxyacetate group by the methoxy ion (stemming from the decomposition of DMFDMA), and then methylation of the resulting phenol by an attack on the methyl group of the dimethyliminium ion (Jerezano et al. 2011; Belov et al. 2011).

In the ^1H NMR spectra of compounds **1–2**, a singlet in the 2.98–3.08 ppm range indicates the presence of dimethylamino protons. The C_2 -H proton of the chromone ring appears as a singlet at around 7.67–8.45 ppm, while the C_3 -H vinyl proton is seen in the 7.15–7.73 ppm range. The full assignment of proton and carbon signals was accomplished by 2D NMR experiments (HMQC and HMBC). Enaminones **1–2** were obtained as a single stereoisomer,

Table 1 Preparation of acyl phenols **6–8**

9a, $\text{R}^1 = \text{OH}$, $\text{R}^2 = \text{OMe}$

9b, $\text{R}^1 = \text{OH}$, $\text{R}^2 = \text{Cl}$

9c, $\text{R}^1 = \text{R}^2 = \text{OMe}$

10a–f

6, $\text{R}^1 = \text{R}^2 = \text{OMe}$

7, $\text{R}^1 = \text{OH}$, $\text{R}^2 = \text{OMe}$

8, $\text{R}^1 = \text{OH}$, $\text{R}^2 = \text{Cl}$

Acyl chloride	R_1	R_2	R_3	Product (%) ^a	δ_{H} (ppm) (HO-2')	δ_{C} (ppm) (C-1)
10a	OMe	OMe	Me	6a (88)	12.65	202.0
10b	OMe	OMe	Et	6b (92)	12.76	204.7
10c	OMe	OMe	<i>n</i> -Pr	6c (85)	12.79	204.3
10d	OMe	OMe	<i>n</i> -Bu	6d (88)	12.78	204.5
10e	OMe	OMe	<i>i</i> -Bu	6e (84)	12.89	204.1
10a	OH	OMe	Me	7a (86)	12.55	201.3
10b	OH	OMe	Et	7b (80)	12.66	204.6
10c	OH	OMe	<i>n</i> -Pr	7c (85)	12.72	204.2
10f	OH	OMe	Bn	7d (50)	12.53	201.3
10b	OH	Cl	Et	8a (99)	12.60	204.8
10c	OH	Cl	<i>n</i> -Pr	8b (90)	12.65	204.4

^aAfter column chromatography

Table 2 Preparation of aryloxy carbonyl compounds **4–5**

7, R¹ = OH, R² = OMe
8, R¹ = OH, R² = Cl

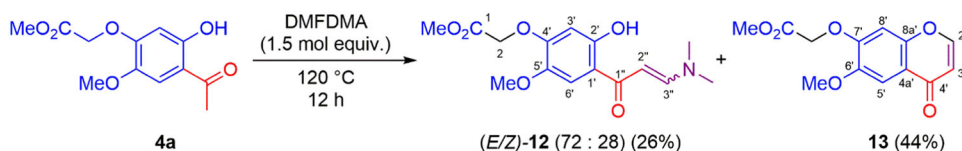
11a-b

4, R⁴ = OMe
5, R⁴ = C₆H₄-4-Cl

Substrate	α -Bromo compound	R ₂	R ₃	R ₄	Product (%) ^a	δ_{H} (ppm) (H-2)	δ_{C} (ppm) (C-1)
7a	11a	OMe	Me	OMe	4a (90)	4.75	168.0
7b	11a	OMe	Et	OMe	4b (97)	4.74	168.1
7c	11a	OMe	<i>n</i> -Pr	OMe	4c (95)	4.74	168.1
8a	11a	Cl	Et	OMe	4d (74)	4.75	167.7
8b	11a	Cl	<i>n</i> -Pr	OMe	4e (80)	4.75	167.7
7a	11b	OMe	Me	C ₆ H ₄ -4-Cl	5a (83)	5.36	191.5
7b	11b	OMe	Et	C ₆ H ₄ -4-Cl	5b (88)	5.36	191.6
7c	11b	OMe	<i>n</i> -Pr	C ₆ H ₄ -4-Cl	5c (70)	5.35	191.6
7d	11b	OMe	Bn	C ₆ H ₄ -4-Cl	5d (80)	5.34	191.5
8a	11b	Cl	Et	C ₆ H ₄ -4-Cl	5e (80)	5.53	191.2

^aAfter column chromatography

Scheme 2 Preparation of *E/Z*-**12** (72:28) and **13** by reacting **4a** with DMFDMA (1.5 mol equiv.)



whose *Z* geometry was established by NOE experiments. The irradiation of the signal assigned to the methyl protons of the dimethylamino group of compound **1b** enhanced the signals corresponding to the aryloxy ring of the chromone scaffold. The same stereoselectivity has been observed in similar systems (Correa et al. 2008; Jerezano et al. 2011; Labarrios et al. 2014), probably due to the greater stability achieved by the planar π -conjugated acrylate system when the bulky dimethylamino group is located at the opposite side of the carbonyl group.

The *Z*-configuration of **1b** was confirmed by X-ray crystallography (Fig. 2). In the crystal lattice, the acrylate system adopts a planar *s-cis* conformation, keeping the oxychromenyl ring system distant from the enaminone moiety and in a noncoplanar conformation [$C(7')-O(C(2)-C(1)) = 81.14^\circ$] with respect to the carbonyl group.

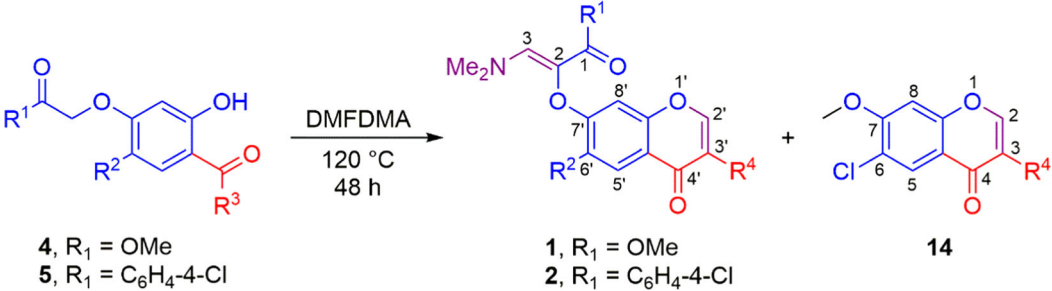
Following the same approach and reacting the corresponding alkyl(*ortho*-hydroxyaryl) ketones **6a–e** with DMFDMA at 120 °C for 12 h, the 3-alkyl chromones **3** were synthesized in good to excellent yields (67–99%, Table 4). When utilizing substrate **6a**, 3-formylchromone **3a** was provided in 67% yield along with by-product **15** in low yield, as a mixture of *E/Z* (85:15). The generation of 3-

formylchromones in low yields has previously been reported when using analogous ketones (Gaspar et al. 2014).

Considering these results and the reports concerning the formation of 3-formyl chromones and enaminones (Gaspar et al. 2014; Correa et al. 2008; Jerezano et al. 2011; Labarrios et al. 2014), a possible mechanism is proposed for the formation of chromonyl enaminones (Scheme 2). Initially, the presence of the methoxy ion promotes the formation of enolate **I** of ketones **4–5**, which reacts with the iminium ion produced by DMFDMA to give species **II**. Demethoxylation of the latter affords species **III**, followed by deprotonation to furnish enaminone **12**, and then an intramolecular cyclization type 6-*exo-trig* converts this into the unsubstituted chromones **13**. For **6a** (R¹=H), a second attack from the iminium ion provides the 3-formyl chromone **3a**. Chromone **13** forms the enolate ketone of the ester group, which attacks the iminium ion to complete the synthesis of chromonyl enaminones **1** (Scheme 3).

α -Glucosidase inhibition activity

α -Glucosidase inhibitors act by delaying glucose absorption, making them potent drugs for the control of blood

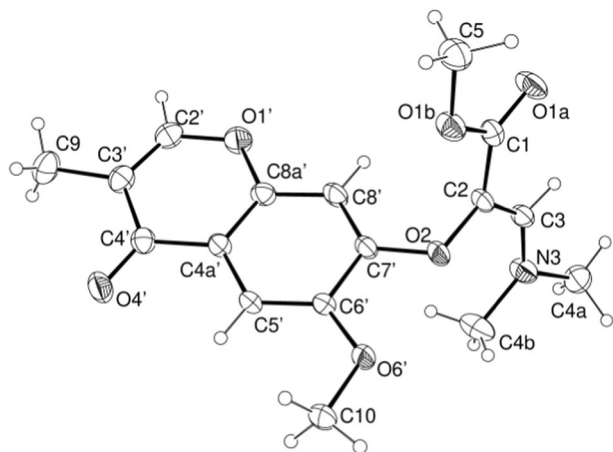
Table 3 Synthesis of chromonyl enaminones **1–2**


4, R₁ = OMe
5, R₁ = C₆H₄-4-Cl

1, R₁ = OMe
2, R₁ = C₆H₄-4-Cl

14

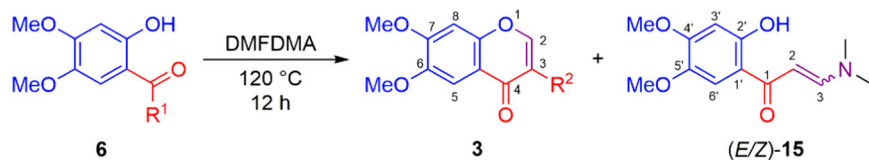
Substrate	R ₁	R ₂	R ₄	Product (%) ^a	δ _H (ppm) (H-3)	δ _C (ppm) (C-3)
4a	OMe	OMe	H	1a (48)	7.21	139.7
4b	OMe	OMe	Me	1b (65)	7.23	139.6
4c	OMe	OMe	Et	1c (48)	7.22	139.7
4d	OMe	Cl	Me	1d (91)	7.24	139.8
4e	OMe	Cl	Me	14a (9)	7.73 (H-2)	151.3 (C-2)
			Et	1e (71)	7.23	139.5
5a	4-Cl-Ar	OMe	CHO	2a (82)	7.15	144.7
			Me	2b (73)	7.16	144.7
5c	4-Cl-Ar	OMe	Et	2c (94)	7.18	144.7
5d	4-Cl-Ar	OMe	Ph	2d (67)	7.17	144.6
5e	4-Cl-Ar	Cl	Me	2e (82)	7.23	144.1
			Me	14a (9)	7.73 (H-2)	151.3 (C-2)

^aAfter column chromatography**Fig. 2** X-ray structure of **1b** (ellipsoids with 30% probability)

glucose levels in diabetic patients (Kerru et al. 2018). Because the chromone scaffold has proved to be a promising ring system for the design and synthesis of new molecules with different biological effects, an *in vitro* determination was herein carried out in relation to the

capacity of the new chromone derivatives **1–3** to inhibit α -glucosidase activity. Acarbose was the positive control (Table 5). Compounds **2a** and **2c–e** were highly active inhibitors (>89.93%, at 10 mM), suggesting a key role played by the 4-chlorophenyl group in the enaminone moiety. Derivatives **1a–e** and **3a–e** did not show significant activity.

The best activity was found when the 4-chlorophenyl was located in the enaminone fragment (i.e., derivatives **2a–e**, of which **2b** exhibited the lowest inhibition). The comparison of the chromonyl enaminones **2a–e** with their chromonyl acrylate analogs **1a–e** revealed that the replacement of the methyl ester by the 4-chlorophenyl ketone significantly increased the activity. According to a recent report, the presence of 4-halophenyl groups in the benzopyran ring favors the inhibition of α -glucosidase (Wang et al. 2018). Interestingly, the highest activity (IC₅₀ = 0.89 mM) was detected for compound **2d** (with a phenyl group at the C-3 position of the benzopyran ring) indicating that a C-3 aryl group enhances this capacity. The structure of compound **2d** without the enaminone fragment is analogous to afmosin, a known natural isoflavonoid, which also exerts

Table 4 Preparation of 3-alkyl chromones **3**


Compound	R ₂	Product (%) ^a	δ _H (ppm) (H-2)	δ _C (ppm) (HC=)
6a	CHO	3a (67)	8.48	159.6
		15 (23)	5.61, 7.85 ^b	89.7, 154.1 ^c
6b	Me	3b (96)	7.74	151.0
6c	Et	3c (98)	7.70	150.8
6d	<i>n</i> -Pr	3d (99)	7.69	151.2
6e	<i>i</i> -Pr	3e (98)	7.67	150.5

^aAfter column chromatography

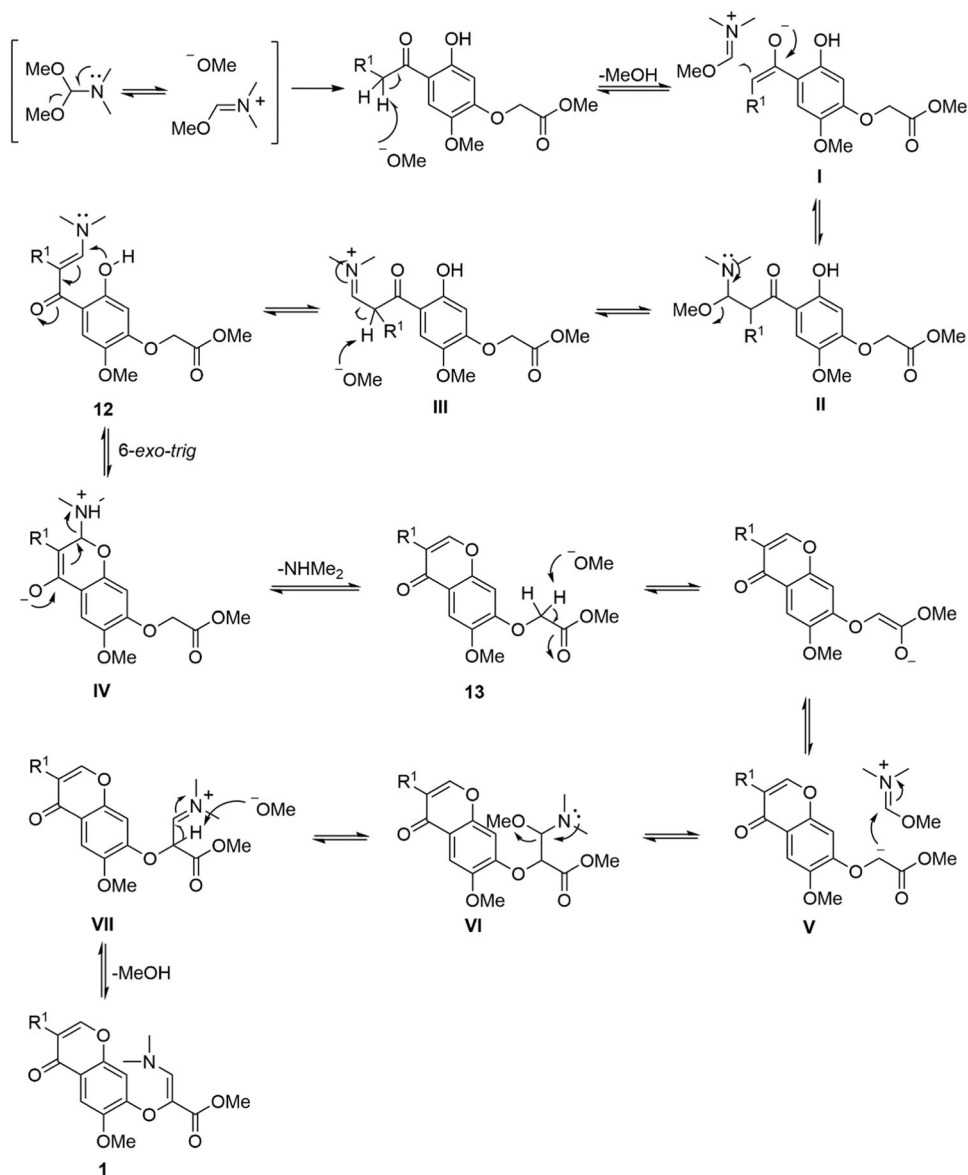
^bδ H-2, H-3 for isomer *E*
^cδ C-2, C-3 for isomer *E*
Scheme 3 Proposal mechanism for the formation of chromonyl enaminones **1** and chromones **12** and **13**


Table 5 DPPH-scavenging and α -glucosidase inhibition found for compounds **1–3**

Compound	% DPPH scavenging activity (10 mM)	% α -Glucosidase inhibition	
		% (10 mM)	(IC ₅₀ mM)
1a	0.0 \pm 0.50	26.93 \pm 0.12	
1b	11.56 \pm 0.74	2.2 \pm 0.06	
1c	16.78 \pm 0.20	17.9 \pm 0.58	
1d	16.05 \pm 0.62	13.6 \pm 0.19	
1e	13.09 \pm 0.85	38.5 \pm 1.00	
2a	43.43 \pm 1.69	89.3 \pm 0.54	5.38 \pm 0.9
2b	14.54 \pm 0.57	33.8 \pm 0.58	11.05 \pm 0.7
2c	6.73 \pm 0.96	92.3 \pm 0.89	8.20 \pm 0.06
2d	10.75 \pm 1.09	93.92 \pm 0.89	0.89 \pm 0.03
2e	0.0 \pm 0.78	93.24 \pm 0.74	1.47 \pm 0.02
3a	18.73 \pm 0.60	22.0 \pm 1.43	
3b	1.30 \pm 0.50	2.8 \pm 0.66	
3c	2.44 \pm 0.33	8.0 \pm 0.96	
3d	1.41 \pm 0.50	9.9 \pm 1.40	
3e	5.60 \pm 0.69	12.1 \pm 0.32	
BHT	85.02 \pm 3.33 ^a	b	
Acarbose	b	63.18 \pm 0.7	7.73 \pm 0.9

^aIC₅₀ = 0.84 mM^bNot determined

an inhibitory effect on the α -glucosidase enzyme (Boonsombat et al. 2017). Therefore, the 4-chlorophenyl group adjacent to the carbonyl group of the π -conjugated enamionone system seems to be very active pharmacophore in the improvement of α -glucosidase inhibition.

Evaluation of the antioxidant activity

Antioxidants are important agents in the prevention of many human diseases, including diabetes mellitus. Oxidative stress plays a pivotal role in the development of diabetes and in the pathogenesis of late diabetic complications (Soengas et al. 2016). Considering, that α -glucosidase inhibitors are potent drugs for treating of diabetes, studies have previously explored the inhibitory capacity of a series of chromones derivatives as well as their radical scavenging activity (Soengas et al. 2016; Takao et al. 2014). To determine the potential of chromonyl enamionones and 3-alkyl chromones **1–3** as antioxidants, all new compounds were assessed for their 2,2-diphenyl-1-picrylhydrazyl (DPPH) free radical scavenging, which was tested by the reduction in color intensity and expressed as the percentage of decrease in DPPH (Table 5). Butylated hydroxytoluene (BHT) served as the positive control. Compounds **1–3** displayed a low level of free radical scavenging.

Compounds **1b**, **1d**, **2a–b**, **2d**, and **3a** exhibited an approximate 10–30% decrease in the DPPH radical. However, no antioxidant effect was found for chromonyl enamionones **1a**, **1c** and **1e**, **2c**, **2e** and 3-alkyl chromones **3b–e**. In summary, the presence of the acrylate or the enamionone fragment in the chromone scaffold showed the best reduction in DPPH.

In vitro antifungal activity

Derivatives of 3-oxyalkyl chromones have been described as promising antimicrobial agents (Dofe et al. 2017a, b). Previous reports suggest that 3-substituted chromones exert a significant activity against *C. albicans* (Chohan et al. 2006, Dofe et al. 2017a, b). Consequently, the 3-substituted chromones **1–3** were herein tested in vitro as possible antimicrobial agents against both standard strains and wild strains of *C. albicans*. This unicellular pathogen is known to cause superficial infections of the oral and vaginal mucosa, which is often disseminated through the bloodstream and deep into tissues, thus producing thousands of deaths in the world annually (Whaley et al. 2017). Azole antifungals (e.g., fluconazole) are often used for the treatment of *C. albicans* infections, but there is growing evidence of the resistance of wild strains of *C. albicans* to these drugs (Canno et al. 2007; Berkow and Lockhart 2017).

Compounds **3c–e** induced significant growth inhibition (MIC, 70–83 μ g/mL) against the fluconazole susceptible strain ATCC[®] 90028. Remarkably, the three chromones showed moderate activity against *C. albicans* (MIC < 300 μ g/mL) and 20 clinical isolates (Table 6), though inhibition of the resistant *C. albicans* strain ATCC[®] 10231 was modest. Regarding the latter strain, compound **3d** displayed the best MIC value, being only four times less effective than fluconazole. Hence, this chromone should certainly be useful as a starting material for designing new more potent analogs.

These data suggest that inhibition of *C. albicans* was significantly enhanced in chromones containing *ortho*-methoxy groups in the aromatic ring but not in those with an enamionone group in the C-7 position of the aromatic ring (not shown in Table 6). Furthermore, antifungal activity is possibly improved by an unbranched aliphatic chain adjacent to the unsaturated γ -pyran ring (Lu et al. 2017; Seleem et al. 2017).

Docking results

The molecular docking results for **2a**, **2d**, and **2e**, the active α -glucosidase inhibitors, are summarized in Table 7. The free energy (ΔG) was lower for compound **2d** than the other two compounds, perhaps due to its aromatic electron-rich

Table 6 In vitro anti-*C. albicans* activity of compounds **3c–e** (MIC \pm SD, $n = 15$, $\mu\text{g/mL}$)

Strain	3c*	3d*	3e*	Fluconazole
ATCC [®] 90028 TM	75.6 \pm 0.04 ^b	70.5 \pm 0.54 ^b	83.1 \pm 0.14 ^a	0.94
ATCC [®] 10231 TM	310.3 \pm 0.21 ^b	287.2 \pm 0.12 ^b	365.4 \pm 0.82 ^a	71.6
1	132.2 \pm 0.12 ^b	74.8 \pm 0.19 ^c	184.2 \pm 0.24 ^a	0.89
2	100.4 \pm 0.03 ^b	84.7 \pm 0.26 ^b	155.7 \pm 0.53 ^a	0.8
3	148.4 \pm 0.24 ^b	76.9 \pm 0.51 ^c	172.9 \pm 0.39 ^a	0.91
4	186.2 \pm 0.27 ^a	85.1 \pm 0.78 ^b	177.3 \pm 0.11 ^a	1.6
5	198.6 \pm 0.14 ^a	126.5 \pm 0.32 ^b	143.7 \pm 0.72 ^b	2.8
6	154.7 \pm 0.75 ^b	111.3 \pm 0.25 ^c	243.8 \pm 0.61 ^a	0.97
7	124.1 \pm 0.17 ^b	88.9 \pm 0.06 ^c	259.5 \pm 0.34 ^a	4.7
8	85.2 \pm 0.43 ^b	73.9 \pm 0.18 ^b	157.5 \pm 0.51 ^a	1.6
9	110.1 \pm 0.18 ^a	95.4 \pm 0.14 ^a	99.6 \pm 0.26 ^a	0.9
10	213.8 \pm 0.41 ^b	153.9 \pm 0.86 ^c	267.8 \pm 0.91 ^a	3.6
11	129.4 \pm 0.08 ^b	87.5 \pm 0.16 ^c	195.6 \pm 0.33 ^b	2.1
12	77.2 \pm 0.11 ^b	70.4 \pm 0.07 ^a	86.9 \pm 0.72 ^a	2.6
13	122.9 \pm 0.74 ^b	115.3 \pm 0.69 ^b	201.2 \pm 0.51 ^a	0.99
14	167.4 \pm 0.16 ^a	99.1 \pm 0.14 ^b	178.3 \pm 0.65 ^a	0.78
15	176.8 \pm 0.63 ^a	121.7 \pm 0.88 ^b	203.6 \pm 0.46 ^a	1.6
16	155.4 \pm 0.31 ^b	107.4 \pm 0.37 ^c	243.5 \pm 0.81 ^a	0.97
17	275.2 \pm 0.13 ^a	174.9 \pm 0.92 ^b	254.3 \pm 0.34 ^a	3.3
18	84.8 \pm 0.27 ^b	72.3 \pm 0.74 ^b	137.5 \pm 0.02 ^a	0.96
19	99.2 \pm 0.53 ^b	84.5 \pm 0.36 ^b	145.5 \pm 0.14 ^a	0.79
20	125.6 \pm 0.86 ^a	86.2 \pm 0.43 ^b	135.8 \pm 0.71 ^a	0.83

*MIC values are expressed in $\mu\text{g/mL}$ and the letters indicate significant differences ($p < 0.05$)

Table 7 Interactions of compounds **2a**, **2d**, and **2e** with residues located in the active site of α -glucosidase

Ligand	ΔG (kcal/mol)	K_i (μM)	Residue involved in ligand recognition
2a	-7.88	1.68	Val100, Asp199, Ala200, Glu256, Trp49, Asn324, Gln167, Tyr63, Asp60, His325, Phe144
2d	-9.37	0.135	Phe280, Phe282, Phe321, Arg197, Trp49, Gln13, Asn324, Phe163, Gln167, Arg407, Asp326, His325, Tyr63, Asn61
2e	-8.56	0.534	Ala200, Glu256, Arg197, Trp49, Asn324, Phe144, Asp326, His325, Gln167, Asp60, Tyr63
Acarbose	-5.45	100.59	Asp199, Arg197, Glu256, Tyr63, Asn61, Asn324, Arg411, Asp60, Asn258, Phe282, Phe144, Arg407, Asp326

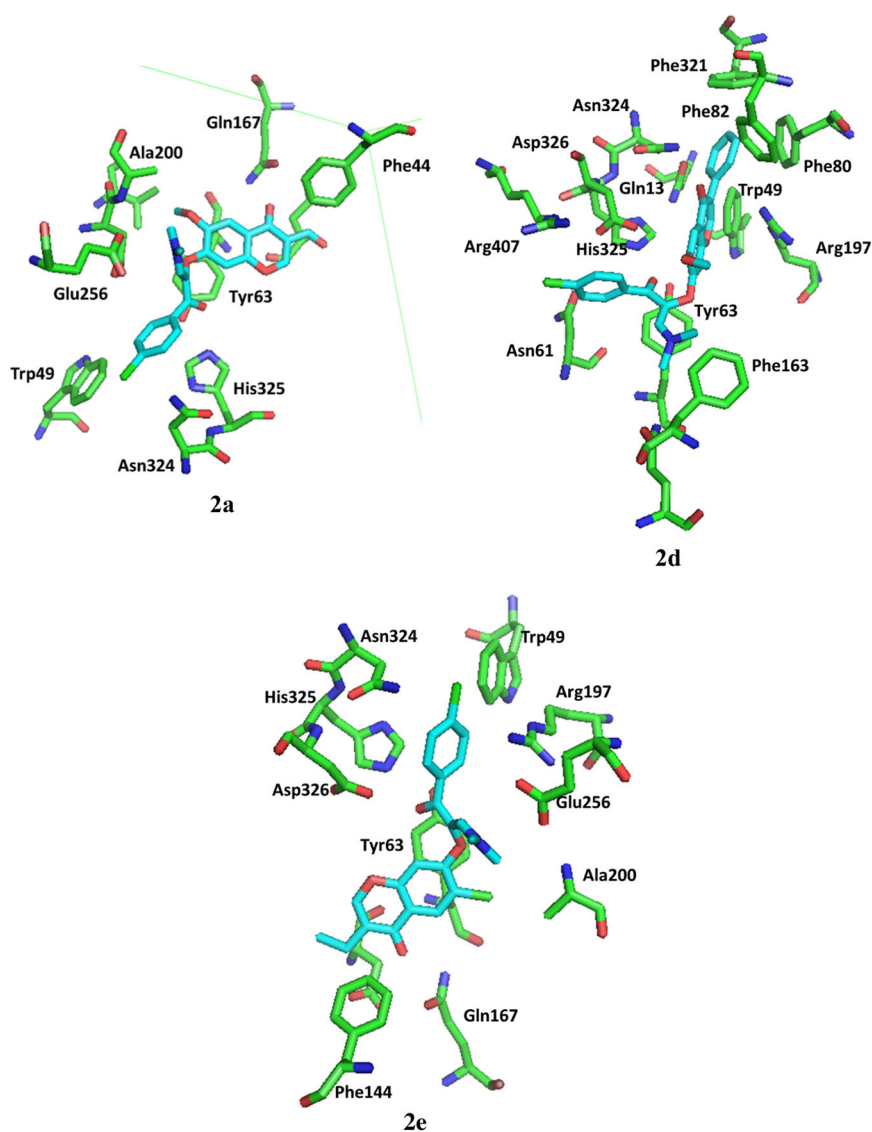
moieties, which may favor the formation of a cluster of aromatic residues and reach Arg residues. This is a plausible explanation for the high affinity of **2d** on α -glucosidase. Analog **2d** interacts with some of the same residues as **2a** and **2e** (Asn324, Gln167, His325, Trp49, and Trp63). It has two more residues in common with **2e** (Arg197 and Arg326), but no more in common with **2a**. However, the latter compound shares additional residue interactions with **2e** (Ala200, Asp60, Glu256, and Phe144). Several residue interactions found in **2d** do not exist in **2a** or **2e** (Phe280, Phe282, Phe321, Phe163, Gln13, Arg407, and Asn61), clearly explaining the differences in stability (ΔG) and affinity for α -glucosidase. The protein–ligand interactions for compounds **2a**, **2d**, and **2e** are illustrated in Fig. 3. Compound **2d** adopts a binding orientation in which the 3-

phenyl ring interacts with the phenyl groups of Phe80, Phe82, and Trp49, further stabilizing the ligand within the enzyme catalytic pocket.

Conclusions

After the series of chromones **1–3** were efficiently synthesized in good yields, they were evaluated as α -glucosidase inhibitors as well as antifungal and antioxidant agents. The biological testing evidenced a different pattern of biological activity for the synthesized derivatives than the standard drugs acarbose, BHT and fluconazole. For example, chromone derivatives **2a** and **2d–e** exhibited good inhibition of the α -glucosidase enzyme (IC₅₀ range of 0.89–5.38 mM),

Fig. 3 Binding modes of compounds **2a**, **2d**, and **2e** in the α -glucosidase binding pocket



better than that of acarbose (IC_{50} of 7.73 mM). The current results suggest that a phenyl group at the C-3 position of the chromone moiety and a 4-chlorophenyl group in the enamionone fragment favored the inhibitory effect on α -glucosidase. On the other hand, no relevant antioxidant capacity (10–30% at 10 mM) was found for any of the test compounds, according to the radical-scavenging assay with DPPH. Additionally, compounds **3c–e** displayed a modest antifungal activity against *C. albicans* strains (IC_{50} range = 70.5–83.1 $\mu\text{g/mL}$). Hence, the antifungal effect was promoted by methoxy groups at the C-6 and C-7 position as well as of an aliphatic chain at the C-3 position of the unsaturated γ -pyran ring. Finally, docking studies revealed that **2d** has the best affinity for α -glucosidase, which is in agreement with the experimental data. Based upon these findings, compounds **2a–e** should certainly be useful as lead

structures for the development of more potent α -glucosidase inhibitors.

Acknowledgements The authors thank Carlos Espinoza-Hicks for help in spectrometric measurements and Bruce A. Larsen for proofreading. J.T. acknowledges financial support from the Secretaría de Investigación y Posgrado, Instituto Politécnico Nacional (SIP-IPN) (grants 20090326, 20100236, 20110172, 20120830, 20130686, 20140858, 20180198, and 20195228) and CONACYT (grants 83446 and 178319). For financial support, F.D. is grateful to SIP-IPN (grants 20170925, 20181332, and 20195287) and J.C.-B. to CONACYT (CBB-254600 and APN-782). A.M.-M. and C.R.-E. thank CONACYT for the graduate scholarships awarded (178319 and 264517) and SIP-IPN (BEIFI) for a complementary scholarship. This work was financially supported by a project from SIP-IPN (20170430, 20181433, 20195786). F.E.J.-M. (20160247), M.C.C.-L. (20160206), F.D., and J.T. are fellows of the Estímulos al Desempeño de los Investigadores (EDI-IPN), and M. C.C.-L., F.D., and J.T. are fellows of the Comisión de Operación y Fomento de Actividades Académicas (COFAA)-IPN.

Compliance with ethical standards

Conflict of interest The authors declare that they have no conflict of interest.

Publisher's note: Springer Nature remains neutral with regard to jurisdictional claims in published maps and institutional affiliations.

References

- ACD/ChemSketch (Freeware) version 14. 01 (2012). Advanced Chemistry Development, Inc., Toronto, ON, Canada
- Belov P, Campanella VL, Smith AW, Priefer R (2011) Microwave-assisted methylation of phenols with DMA-DMF. *Tetrahedron Lett* 52:2776–2779
- Berkow EL, Lockhart SR (2017) Fluconazole resistance in *Candida species*: a current perspective. *Infect Drug Resist* 10:237–245
- Boonsombat J, Prachyawarakorn V, Pansanit A, Mahidol C, Ruchirawat S, Thongnest S (2017) Superbanone, a new 2-aryl-3-benzofuranone and other bioactive constituents from the tube roots of *Butea superba*. *Chem Biodivers* 14:e1700044
- Brunel A-S, Guery B (2017) Multidrug resistant (or antimicrobial-resistant) pathogens—alternatives to new antibiotics. *Swiss Med Wkly* 147:14553–14567
- Canno RD, Lamping E, Holmes AR, Niimi K, Tanabe K, Niimi M, Monk BC (2007) *Candida albicans* drug resistance—another way to cope with stress. *Microbiology* 153:3211–3217
- Cevallos-Casals BA, Cisneros-Zevallos L (2003) Stoichiometric and kinetic studies of phenolic antioxidants from Andean purple corn and red-fleshed sweetpotato. *J Agric Food Chem* 51:3313–3319
- Chin MR, Zlotkowski K, Han M, Patel S, Eliassen AM, Axelrod A, Siegel D (2015) Expedited access to vinaxanthone and chemically edited derivatives possessing neuronal regenerative effects through ynone coupling reactions. *ACS Chem Neurosci* 5:542–550
- Chohan ZH, Rauf A, Naseer MM, Somra MA, Supuran CT (2006) Antibacterial, antifungal and cytotoxic properties of some sulfonamide-derived chromones. *J Enzyme Inhib Med Chem* 21:173–177
- Correa C, Cruz MC, Jiménez F, Zepeda LG, Tamariz J (2008) A new synthetic route of 2-aryl- and 2-benzyl-benzofurans and their application in the total synthesis of a metabolite isolated from *Dorstenia gigas*. *Aust J Chem* 61:991–999
- Csepanyi E, Szabados-Furjesi P, Kiss-Szikszai A, Frensemeier LM, Karst U, Lekli I, Haines DD, Tosaki A, Bak I (2017) Antioxidant properties and oxidative transformation of different chromone derivatives. *Molecules* 22:588–599
- DeLano WL (2002) PyMOL: an open-source molecular graphics tool. *CCP4 Newsletter on Protein Crystallography* 40:82–92
- Dennington R, Keith T, Millan J (2012) GaussView, Version 5. Semichem, Inc., Shawnee Mission, KS
- Dofe VS, Sarkate AP, Lokwani DK, Shinde DB, Kathwate SH, Gill CH (2017a) Novel o-alkylated chromones as antimicrobial agents: ultrasound mediated synthesis, molecular docking and ADME prediction. *J Heterocycl Chem* 54:2678–2685
- Dofe VS, Sarkate AP, Lokwani DK, Kathwate SH, Gill CH (2017b) Synthesis, antimicrobial evaluation, and molecular docking studies of novel chromone based 1,2,3-triazoles. *Res Chem Intermed* 43:15–28
- Farrugia LJ (1997) ORTEP-3 for Windows—a version of ORTEP-III with a Graphical User Interface (GUI). *J Appl Cryst* 30:565
- Farrugia LJ (1999) WinGX suite for small-molecule single-crystal crystallography. *J Appl Cryst* 32:837–838
- Farrugia LJ (2012) WinGX and ORTEP for Windows: an update. *J Appl Cryst* 45:849–854
- Gaspar A, Matos MJ, Garrido J, Uriarte E, Borges F (2014) Chromone: a valid scaffold in medicinal chemistry. *Chem Rev* 114:4960–4992
- Goto H, Terao Y, Akai S (2009) Synthesis of various kinds of isoflavones, isoflavones, and biphenyl-ketones and their 1,1-diphenyl-2-picrylhydrazyl radical-scavenging activities. *Chem Pharm Bull* 57:346–360
- Huls R (1958) Synthesis of substituted chromones. Synthesis of 6,7-dimethoxy-2,2-dimethyl-3-chromene (ageratochromone) *Bull Soc Chim Belg* 67:22–32
- Jerezano A, Jiménez F, Cruz MC, Montiel LE, Delgado F, Tamariz J (2011) New approach for the construction of the coumarin frame and application in the total synthesis of natural products. *Helv Chim Acta* 94:185–198
- Jha HC, Zilliken F, Offermann W, Breitmaier E (1981) Carbon-13 NMR shifts and C–H coupling constants of deoxybenzoin and related acetophenones. *Can J Chem* 59:2266–2281
- Jiménez F, Cruz MC, Zúñiga C, Martínez MA, Chamorro G, Díaz F, Tamariz J (2010) Aryloxyacetic ester structurally related to α -asarone as potential antifungal agents. *Med Chem Res* 19:33–57
- Jhon CH, Riyaphan J, Lin SH, Chia YC, Weng CF (2015) Screening alpha-glucosidase and alpha-amylase inhibitors from natural compounds by molecular docking in silico. *Biofactors* 41:242–251
- Jose ES, Philip JE, Shanty AA, Kurup MRP, Mohanan PV (2018) Novel class of mononuclear 2-methoxy-4-chromanones ligated Cu (II), Zn (II), Ni (II) complexes: synthesis, characterization and biological studies. *Inorg Chim Acta* 478:155–165
- Keri RS, Budagumpi S, Krishna R, Balakrishna RG (2014) Chromones as a privileged scaffold in drug discovery: a review. *Eur J Med Chem* 78:340–374
- Kerru N, Singh-Pillay A, Awolade P, Singh P (2018) Current anti-diabetic agents and their molecular targets: a review. *Eur J Med Chem* 152:436–488
- Kim MK, Yoon H, Barnard DL, Chong Y (2013) Design, synthesis and antiviral activity of 2-(3-amino-4-piperazinylphenyl)chromone derivatives. *Chem Pharm Bull* 61:486–488
- Labarrios E, Jerezano A, Jiménez F, Cruz MC, Delgado F, Zepeda JG, Tamariz J (2014) Efficient synthetic approach to substituted benzo[b]furans and benzo[b]thiophenes by iodine-promoted cyclization of enamines. *J Heterocycl Chem* 51:954–971
- Lu M, Li T, Wan J, Li X, Yuan L, Sun S (2017) Antifungal effects of phytochemicals on *Candida* species alone and in combination with fluconazole. *Int J Antimicrob Agents* 49:125–136
- Mendieta A, Jiménez F, Garduño-Siciliano L, Mojica-Villegas A, Rosales-Acosta B, Villa-Tanaca L, Chamorro-Cevallos G, Medina-Franco JL, Meurice N, Gutiérrez RU, Montiel LE, Cruz MC, Tamariz J (2014) Synthesis and highly potent hypolipidemic activity of alpha-asarone- and fibrates-based 2-acyl and 2-alkyl phenols as HMG-CoA reductase inhibitors. *Bioorg Med Chem* 22:5871–5882
- Moore ML, Day AA, Suter CM (1934) The preparation and germicidal properties of some derivatives of 4-n-butylresorcinol. *J Am Chem Soc* 56:2456–2459
- Morris GM, Huey R, Lindstrom W, Sanner MF, Belew RK, Goodsell DS, Olson AJ (2009) AutoDock4 and AutoDock Tools4: automated docking with selective receptor flexibility. *J Comput Chem* 30:2785–2791
- Musso L, Dallavalle S, Merlini L, Farina G (2010) Synthesis and antifungal activity of 2-hydroxy-4,4-methylenedioxyaryl ketones as analogues of kakuol. *Chem Biodivers* 7:887–897
- Nohara A, Umetani T, Sanno Y (1974) Studies on antianaphylactic agents. I. Facile synthesis of 4-oxo-4H-1-benzopyran-3-carbaldehydes by Vilsmeier reagents. *Tetrahedron* 30:3553–3561
- Philip JE, Shahid M, Prathapachandra Kurup MR, Velayudhan MP (2017) Metal based biologically active compounds: design, synthesis, DNA binding and antidiabetic activity of 6-methyl-3-

- formyl chromone derived. *J Photochem Photobiol B* 175:178–191
- Rao YJ, Krupadanam GLD (1994) Facile synthesis of linear and angular 2-methylfurobenzopyranone. *Bull Chem Soc Jpn* 67:1972–1975
- Reis J, Gaspar A, Milhazes N, Borges F (2017) Chromones as a privileged scaffold in drug discovery: recent advances. *J Med Chem* 60:7941–7957
- Salehi P, Asghari B, Esmaceli MA, Dehghan H, Ghazi I (2013) α -Glucosidase and α -amylase inhibitory effect and antioxidant of ten plant extracts traditionally used in Iran for diabetes. *J Med Plants Res* 7:257–266
- Sarker SD, Nahar L, kumarasamy Y (2007) Microtitre plate-based antibacterial assay incorporating resazurin as an indicator of cell growth, and its application in the in vitro antibacterial screening of phytochemicals. *Methods* 42:321–324
- Seleem D, Pardi V, Murata RM (2017) Review of flavonoids: a diverse group of natural compounds with anti-*Candida albicans* activity in vitro. *Arch Oral Biol* 76:76–83
- Sheldrick GM (2008) A short history of *SHELX*. *Acta Cryst Sect A* 64:112–122
- Sheldrick GM (2015) *SHELXT*—integrated space-group and crystal-structure determination. *Acta Cryst Sect A* 71:3–8
- Soengas RG, Silva VLM, Ide D, Kato A, Cardoso SM, Almeida FAP, Silva AMS (2016) Synthesis of 3-(2-nitrovinyl)-4*H*-chromones: useful scaffolds for the construction of biological relevant 3-(pyrazol-5-yl)chromones. *Tetrahedron* 72:3198–3203
- Sun YL, Bao J, Liu KS, Zhang XY, He F, Wang YF, Nong XH, Qi SH (2013) Cytotoxic dihydrothiophene-condensed chromones from the marine-derived fungus *Penicillium oxacilum*. *Planta Med* 79:1474–1479
- Takao K, Ishikawa R, Sugita Y (2014) Synthesis and biological evaluation of 3-styrylchromones derivatives as free radical scavengers and α -glucosidase inhibitors. *Chem Pharm Bull* 62:810–815
- Upadhyay J, Polyzos SA, Perakakis N, Thakkar B, Paschou SA, Katsiki N, Underwood P, Park KH, Seufert J, Kang ES, Sternthal E, Karagiannis A, Mantzoros CS (2018) Pharmacotherapy of type 2 diabetes: an update. *Metabolism* 78:13–42
- Wang G, Chen M, Wang J, Peng Y, Li L, Xie Z, Deng B, Chen S, Li W (2017) Synthesis, biological evaluation and molecular docking studies of chromone hydrazine derivatives as α -glucosidase inhibitors. *Bioorg Med Chem Lett* 27:2957–2961
- Wang G, Chen M, Qiu J, Xie Z, Cao A (2018) Synthesis, in vitro α -glucosidase inhibitory activity and docking studies of novel chromone-isatin derivatives. *Bioorg Med Chem Lett* 28:113–116
- Whaley SG, Berkow EL, Rybak JM, Nishimoto AT, Barker KS, Rogers PD (2017) Azole antifungal resistance in *Candida albicans* and emerging non-*albicans Candida* species. *Front Microbiol* 7:2173–2184
- Xiu C, Hua Z, Xiao BS, Tang WJ, Zhou HP, Liu XH (2017) Novel benzopyran derivatives and their therapeutic applications: a patent review (2009–2016). *Expert Opin Ther Pat* 27:1031–1045
- Zhen J, Dai Y, Villani T, Giurleo D, Simon JE, Wu Q (2017) Synthesis of novel flavonoid alkaloids as α -glucosidase inhibitors. *Bioorg Med Chem* 25:5355–5364
- Zou H, Jiang H, Zhou JY, Zhu Y, Cao L, Xia P, Zhang Q (2010) Synthesis of 3-(4-hydroxyphenyl)-4-methyl-6-methoxy-7-hydroxycoumarin and its analogous as angiogenesis inhibitors. *J Chin Pharm Sci* 19:136–140